A DATA MINING APPROACH TO PREDICTING PATIENT-BASED LASER MACHINE SETTINGS FOR KIDNEY STONE TREATMENT OPERATION

by

Fidan ESER

B.S., Industrial Engineering, Marmara University, 2017

B.S., Mathematics, Marmara University, 2017

Submitted to the Institute for Graduate Studies in
Science and Engineering in partial fulfillment of
the requirements for the degree of
Master of Science

Graduate Program in Industrial Engineering

Boğaziçi University

2020

ACKNOWLEDGEMENTS

Firstly, I would like to express my deepest gratitude to my advisor Prof. Necati Aras for his patience, guidance, understanding, priceless advice, and kindness at all stages of the process from the beginning to the end. I would like to thank my co-advisor, Prof. Hakan Tozan, who provided his communication network to find answers to the problems I encountered in technical issues, and for his support in many issues from the determination of the thesis subject to the provision of data. It has been a long journey that provides me an opportunity to learn many precious things from my advisors throughout the entire thesis study.

I would also like to thank Prof. Şule Gündüz Öğüdücü and Assist. Prof. Mustafa Gökçe Baydoğan for taking part in my thesis committee and for their valuable comments and suggestions.

Also, I would like to thank Selçuk Güven, Kerem Ertez, and Merve İşler for their help and advice during data processing.

I am also grateful to Prof. Fethi Çalışır for his care about the state of the thesis and his encouragement. I also wish to thank Assist. Prof. Mehmet Ali Ergün for his understanding and good wishes in this process. I would like to extend my thanks to my friends from ITU.

I will never be able to find the correct words to express my gratitude to my family. I am very grateful to my precious sisters Seyhan, Zine, and Elif for their moral support and endless encouragement. Even the presence of them was very important to me.

Thanks to everyone whose name I forgot to mention and who has supported me along the way.

ABSTRACT

A DATA MINING APPROACH TO PREDICTING PATIENT-BASED LASER MACHINE SETTINGS FOR KIDNEY STONE TREATMENT OPERATION

Urinary tract stone disease is a common health problem that affects human health and quality of life. The main goal for the treatment of this disease is to reach a complete stone-free status by causing minimal damage to the patient. The advancement in technology has brought many modalities for the treatment of kidney stones. Selecting the best treatment option by considering patient characteristics is an important factor affecting the success of the treatment. In this study, it is aimed to estimate patient-specific machine settings for successful completion of an operation performed using the Retrograde Intrarenal Surgery method. With this motivation, the performance of linear regression, regression trees, random forest, and extreme gradient boosting methods in machine setting estimation are analyzed. The study is carried out using a dataset provided by the Urology Department of İstanbul Medipol University Hospital. Since the dataset has many missing values with only few complete observations and imputation methods do not provide good results, synthetic data is generated using the original dataset. Models constructed on synthetic data are tested on the original data. Models established on synthetic data have been found to give better estimates. In addition, the models trained on successful observations and the models trained on unsuccessful observations give different estimates, since the data groups they are trained on are different.

ÖZET

BÖBREK TAŞI TEDAVİ OPERASYONUNDA HASTA BAZLI LAZER-MAKİNE AYARLARININ TAHMİNİ İÇİN BİR VERİ MADENCİLİĞİ YAKLAŞIMI

Üriner sistem taş hastalığı, insan sağlığını ve yaşam kalitesini etkileyen yaygın bir sağlık problemidir. Bu hastalığın tedavisinde ana amaç hastaya en az zarar verilerek komplet taşsızlık halinin sağlanmasıdır. Teknolojik gelişmelerle birlikte hastalığın tedavisine yönelik yaklaşımlar çeşitlilik kazanmıştır. Tedavi yöntemlerinin çeşitli olmasının yanı sıra hasta için uygulanması planlanan tedavi yönteminin, hasta karakteristiği göz önünde bulundurularak uygulanması tedavi başarısını etkileyen bir etkendir. Bu çalışmada, böbrek taşlarının RIRS yöntemi ile tedavi edilmesi durumunda operasyonun başarıyla tamamlanması için hastaya özel makina ayarlarının tahmin edilmesi hedeflenmiştir. Bu motivasyonla lineer regresyon, regresyon ağaçları, rassal orman ve ekstrem gradyan arttırma metodlarının makina ayar tahminindeki performansları analiz edilmiştir. Uygulama, İstanbul Medipol Üniversitesi Hastanesi Üroloji Bölümünden sağlanan veri seti kullanılarak gerçekleştirilmiştir. Söz konusu veri setinin, görece az gözlem içermesinin ve uygulanan imputasyon yöntemlerinin başarılı olmamasının, beklenen sonuçların elde edilememesinde etkili olduğu kanısına varılmıştır. Bu sebeple orijinal veri seti kullanılarak sentetik veri üretilmesi yoluna gidilmiştir. Sentetik veri üzerinde kurulan modeller orijinal veri üzerinde test edilmiştir. Sentetik veri üzerinde kurulan modellerin daha az hatalı tahminler verdiği görülmüştür. Ayrıca başarılı ve başarısız alt gruplar üzerinde eğitilen modeller, beklenildiliği gibi üzerinde eğitildikler veri grupları farklı olması sebebiyle birbirinden farklı tahminler vermiştir.

TABLE OF CONTENTS

LIST OF FIGURES

LIST OF TABLES

LIST OF SYMBOLS

$\mathrm{l}(\hat{y}_i, y_i)$	Loss function
$\Omega(f_t)$	Regularization function

LIST OF ACRONYMS/ABBREVIATIONS

ANN	Artificial Neural Network
AUA	American Urology Association
DSS	Decision Support System
EAU	European Association of Urology
ESWL	Extracorporeal Shock Wave Lithotripsy
f-URS	Flexible Ureterorenoscopy
LL	Laser Lithotripsy
LR	Linear Regression
MI	Multiple Imputation
MICE	Multivariate Imputation by Chained Equations
NRMSE	Normalize Root Mean Square Error
PCNL	Percutaneous Nephrolithotomy
RIRS	Retrograde Intrarenal Surgery
RF	Random Forests
RMSE	Root Mean Square Error
RSS	Residual Sum of Squares
SFR	Stone-Free Rate
SWL	Shock Wave Lithotripsy
URS	Ureteroscopic Lithotripsy

1. INTRODUCTION

Kidney diseases, especially nephrolithiasis (kidney stones), are prevalent among people all over the world [16]. Around 12% of the world population suffers from urinary tract stones [17]. Males, people with obesity, and patients with diabetes are more likely to face urolithiasis [18]. The kidney stone disease, which occurs in 5-6% of females and 10-12% of males, is a common health issue in the Western world [19]. According to the studies, it is estimated that 600,000 people experience kidney stones annually in the United States [20]. 50% of kidney stone disorders seen in 12% of the Indian population result in loss of kidney function or kidney damage [20].

The advancement in technology has brought many modalities for the treatment of kidney stones. In the past, patients with kidney stones were treated with open surgery. There are several available methods for lithotripsy including Extracorporeal Shock Wave Lithotripsy (ESWL), Percutaneous Nephrolithotomy (PCNL), and currently Retrograde Intrarenal Surgery (RIRS).

ESWL and RIRS are among the most common treatment options for ureteral stones [21]. Nevertheless, the type of the treatment that depends on the stone placement, size, and chemical properties differ from patient to patient [22]. The size of the stone is the most significant among these, because it heavily affects the stone-free rate (SFR) [23].

RIRS, which is applied under anesthesia, involves the placement of a fine viewing tube–known as fiberoptic endoscope–through the urethra, beyond the bladder and up to the stone in the ureter or kidney [24]. Thus, the endoscope is moved retrograde (up the urinary tract system) to within the kidney (intrarenal). In this treatment modality, the stones are divided into small pieces using a laser, and larger fragments are removed by a basket. Following this stage, a stent (hollow thin tube) is placed in the ureter to prevent kidney obstruction. Then, the stent can be removed by a minor operation.

Achieving a high success rate and accessing the stone through a natural route have made RIRS a significant and extensively used treatment method [25]. The advancement of half and flexible ureteroscopes, smaller caliber, and the introduction of enhanced devices have made URS more powerful and admissible for the treatment of stones in all pieces of the urinary tract [26].

In 1964, Marshall reported the first usage of f-URS [27]. The use of f-URS has accelerated in the late 1980s with the introduction of a device with an irrigation channel and a flexible tip [25]. In 2004, digital f-URS has been launched to the market enhancing the quality of image compared to the fiberoptic f-URS [28].

The present laser lithotripters allow users to adjust multiple parameters that contain pulse duration, pulse energy (J), and pulse frequency (Hz) [28]. Although the determination of the most appropriate technique depends on factors such as the stone size, surgeon preference, stone composition and location, these techniques can be combined during the same process to obtain better results [28]. However, it can be a hard task for urologists to decide on the settings of laser lithotripter for optimal use. The power, which is one of the machine settings, increases heat production in the environment as its level increases. The heat generated in the environment due to high power can cause thermal tissue damage [29].

In this study, laser machine settings are tried to be estimated in order to achieve high success in the treatment of patients diagnosed with stones. These settings are unique for each patient. Pre-operative and some peri-operative variables belonging to the patients are processed in the R program using a few techniques from data mining.

The remaining part of this thesis is structured as follows. In Section 2, the literature related to kidney stones is reviewed. In Section 3, methodologies used in this study are explained. In Section 4, the data used in the study and the results of the methods are presented. Finally, conclusions of the study are stated in Chapter 6.

2. LITERATURE REVIEW

Salt and minerals accumulated in the urine form hard masses of kidney stones. Under normal conditions, the minerals and salt dissolved in the urine are removed from the urinary tract without any problem. However, when urine becomes more concentrated with higher levels of certain minerals, stone formation is observed. The chemical composition of kidney stones varies according to the ratio of various chemicals in urine [30]. According to alterations in the mineral composition, kidney stones are divided into several groups [31]. Although kidney stones usually appear in kidneys, they might pass lower down in the urinary tract, which consists of three parts: bladder, ureters, and urethra [32].

A stone formation that does not have any symptoms at first, results in symptoms such as urinary tract infections, flank pain (pain in the backside), hydronephrosis (dilation of the kidney), and blockage of urine flow as time progresses [33].

Kidney stone, a kidney disease that is common among people all over the world, affects about 12% of the world's population [17]. Men, people with obesity, and patients with diabetes are more prone to encounter urolithiasis [18]. Urinary system stone disease, which is 1.5 times more common in men than in women, is a common health issue in the Western world [19]. According to the studies, it is estimated that 600,000 people experience kidney stones per year in the United States [20], while 50% of kidney stone disorders seen in 12% of the population of India cause loss of kidney function or kidney damage [20].

The increase in the prevalence of kidney stone disorders in recent years is attributed to warm climates (fluid loss) and lifestyle characteristics such as lack of physical activities [34]. The formation of stones might be caused by genetic factors, and also depends on geographical factors and age [35].

The advancement of technology has brought many alternatives for the treatment of kidney stones. Kidney stones treated with open surgery in the past are treated with alternative methods such as ESWL, RIRS, and PCNL.

2.1. Extracorporeal Shock Wave Lithotripsy (ESWL)

ESWL, which is a non-invasive method, has been used as a treatment method since the early 1980s [36]. In this treatment, the stones are broken with shock waves, which are produced by a device called lithotripter. After the ESWL treatment, the small pieces of stones are excreted in the urine. The goal of ESWL treatment is to maximize the fracture of the stone by giving the least damage to the kidneys and nearby tissues. In an ESWL process, the urologists are interested in three parameters: voltage (or energy) of the shock wave generator, the number of shock waves applied, and the repetition rate [37].

The stone size and the SFR of ESWL treatment are inversely proportional. Since the SFR is not sufficient for stones with a diameter of 2 cm, ESWL is a method used in stones with a diameter less than 2 cm [38].

Factors that reduce the success of ESWL [39] are

- Stones larger than 3 cm,
- Existence of multiple stones,
- The presence of stones in the localization of the lower pole calyx,
- Large skin-stone distance,
- Hounsfield units(HU), which stands for the hardness of the stone, with a value more than 1000, and
- Obesity.

Abdel-Khalek *et al.* [40] study to determine the factors that are effective on SFR of post-ESWL. Using multivariate analysis, they identify the important factors as the stone location, stone size, and existence of ureteric stent. They also design a logistic

regression model that helps to select the appropriate patients for ESWL.

Choo *et al.* [41] apply a machine-learning algorithm to analyze the factors that determine the success of a single-session ESWL in ureter-stone cases. In order to determine the probability of treatment success, they develop a 92.9% accurate decision support model consisting of 15 parameters. As a result of this study including 791 patients, they find the success rate of single-session ESWL to be 64.4% (509). The success rates are found to be 59.8%, 65.5%, and 69.6% for upper, middle, and lower ureteral stones, respectively.

In a study, where the cost-effectiveness of ureteroscopic lithotripsy (URS) versus ESWL is evaluated, it is shown that URS provides more SFR for the ureteral stones than ESWL [21]. Besides, the decision analysis model that exists in the study demonstrates that ESWL is not a cost-effective alternative when SFR of ESWL is less than 60-64% or URS has an SFR greater than 57–76%.

2.2. Percutaneous Nephrolithotomy (PCNL)

Percutaneous nephrolithotomy (PCNL) treatment, which emerged in the 1980s [42], is preferred to treat stones larger than 2 cm or ESWL-resistant stones [43]. In this method, which is applied under anesthesia, the stones that are broken by laser are taken out utilizing a device placed in an incision opened in the skin. While PCNL is preferable for stones larger than 2 cm, staghorn, partial staghorn stones, it has contra-indications such as bleeding disorders, pregnancy, and uncontrolled urinary tract infections [44].

PCNL, which is proposed as the first option for treatment of stones greater than 2 cm in the 2017 European Association of Urology (EAU) guideline, has SFR up to 95% [44]. It is found to be more effective in the treatment of 20-30 mm single renal pelvic stones, whereas ESWL has fewer complications and causes a lower cost for the same cases [23]. Although PCNL is an effective modality in the treatment of renal calculi, it might cause kidney damage and various complications [45]. The drawbacks of standard PCNL–compared to RIRS and ESWL–include greater pain,

longer hospitalization duration, and an increase in bleeding [46].

The risk of PCNL complications is connected with the diameter of the device used in operation [47]. Since the optimal stone treatment method requires a combination of the high SFR of PCNL and the low morbidity of ESWL, studies on miniaturization of PCNL are performed. The main purpose of these studies is to minimize the cross-section of the nephroscope used in PCNL [48].

Bagcioglu *et al.* [49] conduct a study to analyze the cost of micro-percutaneous nephrolithotomy (microperc) and RIRS. The cost that is audited includes the cost of hospitalization, devices, additional required treatments, and disposables. At the end of the statistical analysis performed in the study, it is found that the use of microperc is less expensive than RIRS due to additional required treatments and auxiliary equipment in RIRS. Besides, one of the results obtained in this study supports the efficacy of RIRS for the duration of the operation.

Aminsharifi *et al.* [50] developed an Artificial Neural Network (ANN) system that predicts different outcome variables of PCNL. In this study, a dataset that includes pre-operative and post-operative data belonging to 200 patients are used as a training set to examine how the pre-operative values affect the post-operative variables. Stone morphometry and stone burden are shown to be among the most important pre-operative features affecting all post-operative outcome variables.

Treatment of kidney stone disorders requires many parameters to be considered. A treatment procedure is multi-factorial. Therefore, a decision support system (DSS), which can help surgeons predict the outcome of treatment and decide on the appropriate treatment method, can be efficient in lessening the potential risks of treatment. Shabaniyan *et al.* [51] create a promising DSS to provide consultancy before the operation. The developed DSS is promising for estimation of post-operative outcome of a kidney stone treatment operation, especially for PCNL.

2.3. Retrograde Intrarenal Surgery (RIRS)

In 1854, the physicist John Tyndall was able to bend the light in a flexible glass, the light was propagated through the glass fiber. The first usage of ureterorenoscope was declared in 1929 by Young and McKay [52]. Since the first ureteroscope did not have active deflection ability and a working channel, it was used only for diagnostic purposes [52, 53]. In 1980, the first rigid ureteroscope with a working channel was developed by Karl-Storz. In the same year, Bagley and his colleagues laid the foundations of F-URS by adding technical features such as passive and active deflection to the ureteroscope [54, 55]. The use of f-URS has accelerated in the late 1980s with the introduction of devices with an irrigation channel and a flexible tip [25].Thus, the kidney stone treatment by retrograde route has gained speed.

Retrograde intrarenal surgery (RIRS), which is applied under anesthesia, is a procedure that involves the placement of a fine viewing tube (known as fiberoptic endoscope) through the urethra, beyond the bladder and up to the stone in the ureter or kidney [24]. Thus, the endoscope is moved retrograde (up the urinary tract system) to within the kidney (intrarenal). In this method of treatment, the monitored stones are divided into small pieces using a laser and larger fragments are removed by a basket. After this stage, a stent (hollow thin tube) is placed in the ureter to avoid kidney obstruction. Then, the stent can be removed by a minor operation. This treatment is an alternative modality for patients with kidney anomalies, morbid obesity, and ESWL failure [56].

In present, using digital flexible ureterorenoscopes with a thinner and wider working channel, the development of endoscopic devices, the use of holmium laser lithotripsy in the treatment of renal calculi have increased the success rate of the RIRS treatment method and the complication rates resulting from treatment have been reduced [57,58].

Achieving a high success rate with low morbidity and accessing the stone through a natural route have made RIRS an important and widely used treatment method [25]. The development of smaller caliber, half and flexible ureteroscopes, and the introduc-

tion of improved devices, including the Ho:YAG laser (an effective stone crusher), have made ureteroscopy (URS) safer and more effective for the treatment of stones in all parts of the ureter [26].

RIRS surgical technique is prone to change due to advances in technology. The equipment produced parallel to the advancements in technology has the potential to reduce the cost/benefit ratio as well as the complication rate that may arise due to the operation [25]. The main instruments used in RIRS are briefly summarized below.

- Flexible Ureterorenoscope

  Flexible ureterorenoscopes mainly consist of three parts: optical system, bending mechanism, and working channel (Figure 2.1). The optical system can be digital or fiberoptic [59]. Fiberoptic ureterorenoscopes generally have a sandy image [60]. Digital f-URS have been developed to obtain better quality images and they achieve this by providing real-time images through the optical chip on their ends [61].

  Both types of f-URS are prone to degradation by their delicate nature. f-URS may be impaired due to misuse, such as the surgeon firing the laser inside the device or forcing it to over-deflection in the wrong position [62]. In addition, changes such as duration of use, operation time, number of ureteral accesses, lower pole operation time, auxiliary instrument usage time also affect the durability of the device [63].

Figure 2.1. Flexible Ureterorenoscope [1].

- Ureteral Access Sheath (UAS)

  UAS, which is started to be used in RIRS operations after 2000, was first developed by Takayasu and Aso in 1974 [64, 65]. The equipment used to facilitate the entry into the kidney collecting system reduces the damage that may occur in f-URS in repeated entries, decreases the cost, reduces the operation time, and increases the surgical success [32, 66]. On the other hand, some studies have shown that UAS causes post-operative ureteral edema and requires post-procedure DJ stents [67].

  In a study conducted by Traxer *et al.* [68], it is indicated that using UAS during f-URS to remove stones is safe, but has no significant effect on post-operative SFR.

Figure 2.2. Ureteral Access Sheath [2].

  UAS, shown in Figure 2.2, may not be necessary for kidney stones where all stones can be broken in one go. However, in cases where it is necessary to extract more than one piece, repeated entries of f-URS can be done easily and safely using UAS [67].

- Guidewire

  Guidewires are used to facilitate the access of semirigid and flexible ureterorenoscopes to the upper urinary system [69]. In a study conducted by Ulvik et al. [70], it has been observed that the use of safety guidewire provides significant benefit

during the placement of ureteroscope. Since a flexible tip facilitates a maneuver around the stone, the ideal guidewire should have a flexible and soft tip [69]. In addition, its slipperiness and stiff body are other important factors that facilitate the placement of a UAS or stent [25]. Despite these advantages and benefits, there is a possibility of ureteral injury during the use of guidewires.

- Basket Catheter

  Basket catheter is an auxiliary equipment used in both rigid and flexible ureterorenoscopy to remove fragmented stone pieces or to move the stone [69]. It consists of wires resembling a cage at the distal end (shown in Figure 2.3).

  Placing the stone in a more convenient place with a basket catheter before starting to break the stone during f-URS will reduce the risk of damage to the ureterorenoscope [69].

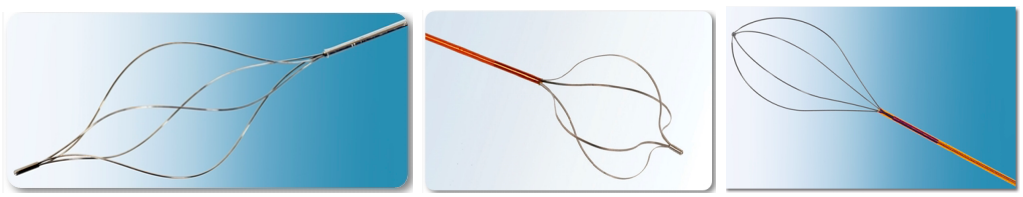

(a) Helical basket (b) Flatwire basket (c) Tipless basket

Figure 2.3. Three different forms of basket catheters [3].

  Basket catheters with helical shapes are opened and rotated behind the stone to grab the stone. The most suitable stone extraction device in RIRS made with a flexible ureterorenoscope is a tipless basket [71]. Due to its success and ease of use, tipless nitinol basket catheters are preferred more frequently to grab stones in the calyx or renal pelvis [25, 72].

- Double J Stent

  Double J (DJ) stent is a device that facilitates the passage of urine from kidney to the bladder with a J-shaped curve at both ends. This equipment (illustrated in Figure 2.4), which is used by many surgeons as a routine part of ureteroscopy, is mostly used to prevent remaining stone fragments from blocking the kidney

and to repair small-scale ureter damage occurring during the surgery [73].

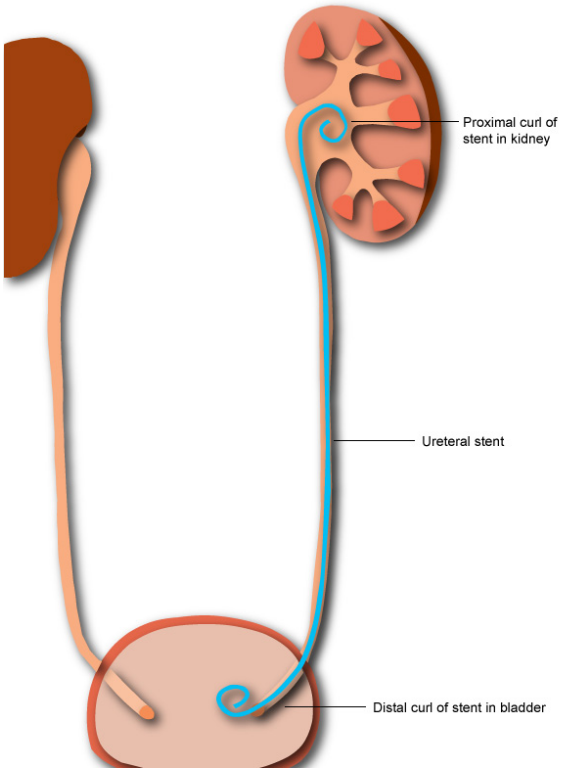

Figure 2.4. DJ stent placement [4].

- Laser Lithotripsy (LL)

  Laser lithotripsy is used in f-URS. The thin and flexible laser fibers make the laser energy the ideal stone breaking method for the f-URS process. The most used laser type is Holmiyum-YAG laser (Ho:YAG) [57, 74].

  Ho:YAG laser was introduced in the early 1990s [75]. It is a pulsed laser type, meaning that laser energy is generated and used in a series of pulses instead of a continuous energy beam [76]. Thus, it causes less damage to the surrounding tissues and provides more effective use of laser energy [76]. It is absorbed by the water molecules that make up a significant part of the structure of the stones. As a result of the application of laser energy, the chemical structure of the stone deteriorates, its tension decreases ,and the stone breaks as a result of evaporation of the water in the stone [77]. Since it does not affect the stone mechanically but affect thermally, it ensures that the stone is broken without causing migra-

tion [78]. Besides all these advantages, there are some disadvantages such as high cost, potential to damage the ureter and endoscopic instruments, and long working time [79].

The thing that makes LL a proposed ureteroscopic energy source by the American Urology Association (AUA) and the European Urology Association (EUA) is its compatibility with rigid, semi-rigid, and flexible ureteroscopes [80].

The present laser lithotripters enable the urologists to set up some parameters: pulse energy (J), pulse frequency (Hz), pulse duration, and consequently total power, which is obtained by the product of pulse energy and pulse frequency [7,28] (see Figure 2.5).

Figure 2.5. Laser parameters [5].

Basketing and dusting are two alternatives for the fragmentation of stones with LL. In the "basketing", stones that are fragmented into smaller pieces by using high-power and low-frequency laser settings are removed. "Dusting", on the other hand, involves the utilization of low-power, high-frequency laser pulses to fragment stones into powder-like pieces that can pass through the urine spontaneously [81]. Another setting named "popcorn effect" might be utilized after the basketing to produce smaller pieces of fragments [79].

Keller *et al.* [28] have specified laser settings for these techniques as follows:

- Popcorn effect: High frequency (1 J) and high energy (10-20 Hz).
- Basketing: High frequency (1-2 J) and low energy (3-5 Hz).
- Dusting: low frequency (0.2-0.5 J) and high energy (10-20 Hz).

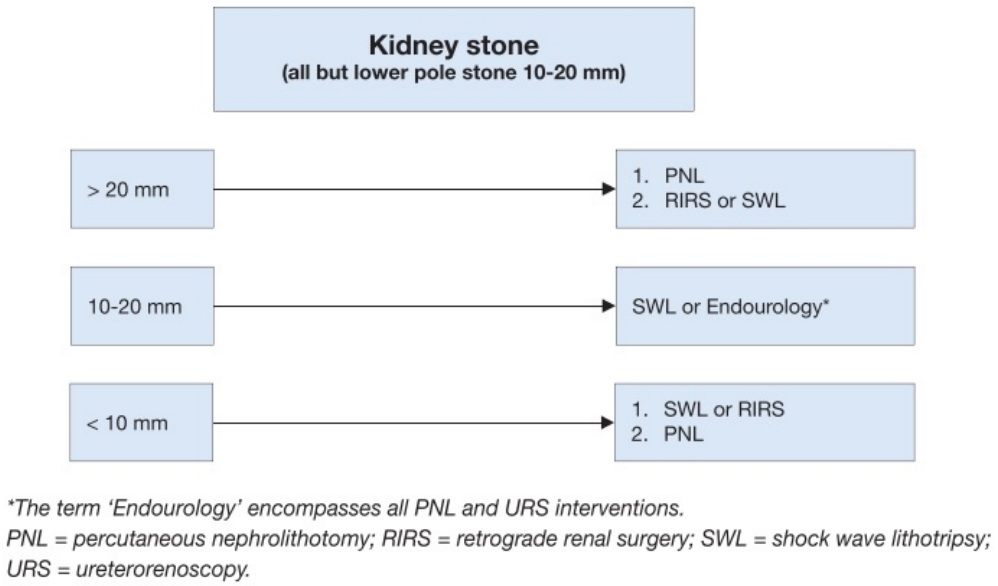

Figure 2.6. Treatment algorithm for renal calculi [6].

Although the determination of the most appropriate technique depends on factors such as the stone size, stone composition, stone location, and surgeon preferences, these techniques can be unified during the process to obtain superior results [28].

Urologists' preferences regarding laser setting for LL do not follow the same pattern. A questionnaire is applied to an international group of urologists at the World Endourology Congress to make an understanding of patterns in the laser machine settings preferences of urologists [82]. In this study, 136 participants were asked about the laser preferences they applied to the treatment of proximal ureter stones. The results show that the general preferred laser setting is 0.8 J and 10 Hz.

The application of the aforementioned LL techniques depends on the characteristics of the stone and its location. Sarah *et al.* [83] provide the optimum settings for

several lithotripsy techniques, considering the characteristics of stones.

The results of numerous studies in the literature show that the use of Ho:YAG lithotripsy at low pulse energy generates fragments smaller than 1 mm at a slow fraction rate, while its use in higher pulse energy forms greater fragments at a quicker fraction rate [84–87]. Sea *et al.* [88] irradiate phantom stones with Ho:YAG to investigate the effect of factors such as pulse energy, pulse frequency, and retropulsion on the efficiency of lithotripsy. In the study where 6 different settings are tested, stabilization devices were shown to be more effective, especially in high pulse energies.

One of the conducted studies [88] shows that, in general, low pulse energy produces smaller fragments and minimizes stone retropulsion, but increases operation time. In laser lithotripsy, besides the aim of successfully ending the operation, another important goal is to complete the operation as quickly as possible. Previous findings have shown that the use of high pulse energy ends the operation faster [89, 90]. However, a high pulse energy setting causes an increase in retropulsion [91]. Larger fragments resulting from the preference of high pulse energy might necessitate the basketing process and raise the cost depending on basket usage [88]. In addition, high pulse energy brings about fiber tip degradation, which leads to a decrease in fiber lifetime [92]. Since this degradation in the fiber tip reduces the amount of energy reaching the stone, it can reduce fragmentation efficiency, increase operation time, and increase cost due to the replacement of the fiber [29].

Although some laser lithotriptor manufacturers claim that the high-frequency setting is more ablative [93], several studies have shown that the increase in pulse frequency does not have a significant effect on the ablation volume [79, 88]. In a recent study in which the total power was kept steady, a linear relationship was detected between pulse energy and ablation volume [7].

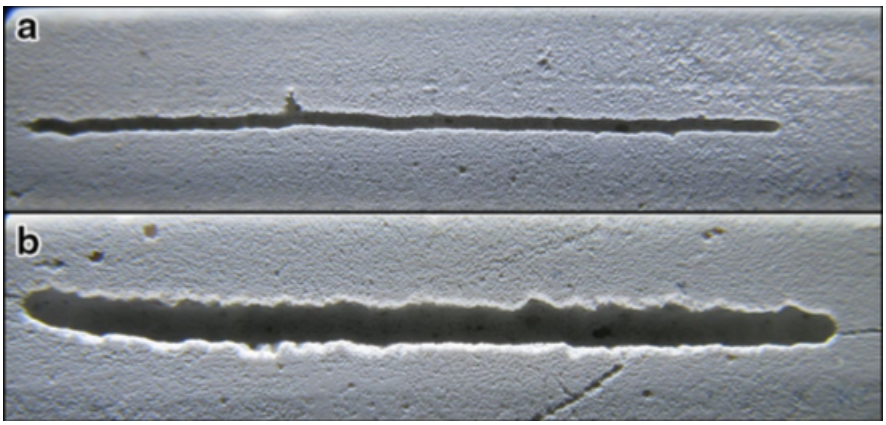

Figure 2.7. Comparison of the outcomes of different lithotripter settings by keeping the total power constant and using the identical laser fiber: a) 30 Hz × 0.2 J (high frequency-low pulse energy) b) 5 Hz × 1.2 (low frequency-high pulse energy) [7].

The new lithotriptor models offer the new long-pulse form alongside the traditional short-pulse form, allowing urologists to choose different pulse duration [7]. The energy conveyed by a single laser pulse is distributed over a longer period of time in the long pulse form compared to the short pulse mode [7]. As a result of the experiment conducted on the artificial stones, Kronenberg and Traxer conclude that the long-pulse form is considerably less ablative than the short-pulse one.

It is important to accomplish a stone-free status after the operation to prevent incidents arising from residual stones [94]. Numerous studies are carried out to determine factors contributing to the stone-free status after the operation. The first of these studies, carried out by Ito *et al.* [94], shows that the number of stones, lower pole stones, and the presence of hydronephrosis are predictive factors for the post-operative stone-free status. In another study conducted by Tonyalı *et al.* [95], the use of UAS is shown to be one of the most significant predictors for the prediction of stone-free status after RIRS.

A string of scoring systems has been constructed to estimate the SFR after the operation. Resorlu *et al.* [96] report a scoring system for the probability of stone clearance. Later, Jung *et al.* establish a score that does not consider stone burden and

numbers [97], although the stone burden is considered as an indispensable indicator for the SFR [98, 99]. Xiao *et al.* [100] develop a more comprehensive scoring system that takes the stone burden into account and ranges from 4 to 10.

As mentioned above, there are various studies in the literature regarding the laser treatment of kidney stones. These studies are very diverse and cover topics such as laser fibers, laser lithotripters and related complications, laser settings and techniques [101]. However, as far as we know, no study has been carried out to date, offering a specific laser machine setting for each stone case. In this study, the pre-operative and some peri-operative data belonging to patients, who come with the complaint of stone in the urinary system are analyzed. Personalized laser settings are provided using data mining techniques.

3. METHODOLOGY

A regression problem is a prediction problem in which the dependent variable is continuous quantitative variable. Estimating the price of a house based on some characteristics of the house or estimating daily electricity consumption for a region are examples for regression problems.

This study aims to determine patient-based machine settings for an RIRS operation to be completed successfully. An operation that ends in a stone-free status is described as successful. Since the current dataset contains two parameters of machine setting, i.e. power and frequency, two different predictions are made. For this purpose, firstly, each observation in the dataset is labeled by the guidance of a field expert. Observations with a successful treatment are labeled as "success", while those that do not satisfy the condition for a successful operation are labeled as "failure". The labeled observations are divided into two groups according to their success status. After this phase, data mining algorithms are performed on these two subgroups. In other words, two models have been constructed for each subgroup using a data mining method: one for frequency and one for power setting estimation. Models trained on successful cases and models trained on failed cases are expected to give different estimates for machine settings. In conclusion, the constructed models' predictions for the successful (unsuccessful) completion of an operation are expected to be different.

In this section, forecasting methods that are used and evaluated in this thesis are summarized.

3.1. Linear Regression

The linear regression method is used to estimate the value of a continuous variable by the value(s) of other continuous and categorical variable(s). In this technique, a linear mathematical model is used to explain the relationship between two (simple

linear regression) or more variables (multiple linear regression).

$$Y = \beta_0 + \beta_1 X_1 + \beta_2 X_2 + ...\beta_p X_p + \epsilon \tag{3.1}$$

where,

$$\begin{cases} Y & : \text{dependent variable or target/response} \\ X_i & : \text{independent variables} \\ \epsilon & : \text{error} \end{cases}$$

In practice, $\beta_1, \beta_2, ..., \beta_p$ (so called regression coefficients) are not known and need to be estimated from the given data. By using the estimated $\hat{\beta}_1, \hat{\beta}_2, ..., \hat{\beta}_p$, predictions can be made by the following formula

$$\hat{y} = \hat{\beta}_0 + \hat{\beta}_1 x_1 + \hat{\beta}_2 x_2 + ...\hat{\beta}_p x_p. \tag{3.2}$$

Linear models are fitted by minimizing the sum of squared residuals between fitted values and real values. $\hat{\beta}_1, \hat{\beta}_2, ..., \hat{\beta}_p$ are chosen in such a way that they minimize the RSS in Equation 3.3.

$$RSS = \sum_{i=1}^{n} e_i^2 = \sum_{i=1}^{n} (y_i - \hat{y}_i) = \sum_{i=1}^{n} (y_i - \hat{\beta}_0 - \hat{\beta}_1 x_{i1} - \hat{\beta}_2 x_{i2} - ... - \hat{\beta}_p x_{ip})^2 \tag{3.3}$$

3.2. Regression Tree

A decision tree is an efficient method for both the regression and classification problems. It consists of a root node, a group of internal nodes, and a set of terminal nodes. The basic concept is to split a complex decision into several simpler ones, which may provide a more interpretable solution [102].

A regression tree, which is a variant of decision trees, is an algorithm where the target variable is continuous. On the contrary, when the target variable is discrete, it is named a classification tree.

The process of creating a regression tree follows a greedy approach known as binary recursive partitioning. In this process, all the observations that are initially grouped into the same region are divided into separate regions by considering every possible binary split on each variable (region). For the variable X_j and cut point c, the region is partitioned as shown in Equation 3.4. The algorithm determines X_j and c that yield the lowest residual sum of squares (RSS) (shown in Equation 3.5 where $\hat{y}_{R_1}$ and $\hat{y}_{R_2}$ represent the mean of the output variable for the observations in $R_1(j, c)$ and $R_2(j, c)$ respectively) [103]. The splitting rule is performed on each newly obtained branch. This process continues until each node meets the conditions set by the user. Nodes that satisfy user-specified conditions are called terminal nodes.

$$R_1(j, c) = \{ X : X_j < c\} \quad \text{and} \quad R_2(j, c) = \{ X : X_j \geq c\} \tag{3.4}$$

$$\sum_{i:x_i \in R_1(j,c)} (y_i - \hat{y}_{R_1})^2 + \sum_{i:x_i \in R_2(j,c)} (y_i - \hat{y}_{R_2})^2 \tag{3.5}$$

There are several parameters that may have an impact on the quality of predictions. A few of these parameters are depth of the tree, the minimum number of samples required to split, and the minimum number of samples existing at a leaf node [104]. The depth specifies the complexity of the tree. A deeper tree represents more splits and catches more information about the data. The models created by trees with a high depth fit perfectly to the training data, however, cannot generalize well for unseen data.

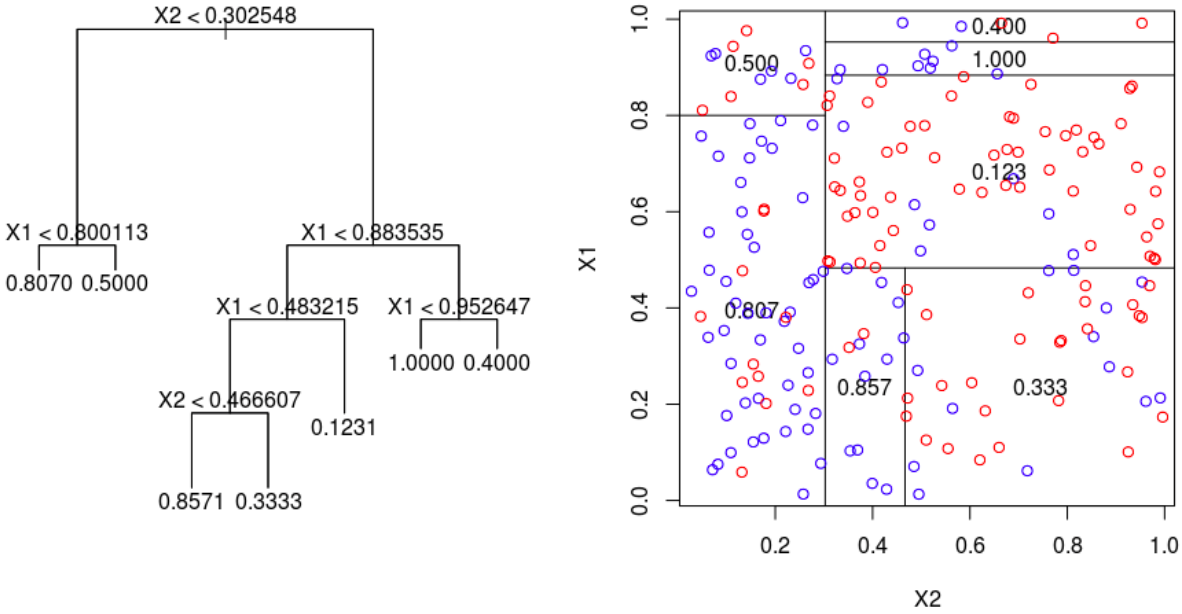

Figure 3.1. Regression tree [8].

3.3. Random Forests

Random Forests are an advantageous ensemble learning method that can be used for both classification and regression problems. Bootstrap aggregating method (bagging) is utilized for building a series of trees. During the building of these trees, Random Feature Selection method comes into play. Random Feature Selection decorrelates trees by splitting each node based on a random sample of m predictors chosen from the complete set of M predictors. In this manner, RF provides an improvement over bagging.

A process, called voting, is carried out to forecast a new instance. For regression problems, the average of prediction of each tree is taken as the ultimate estimate, while the majority vote for classification problems is chosen as the final result. Figure 3.2 briefly explains the prediction process of the random forest algorithm.

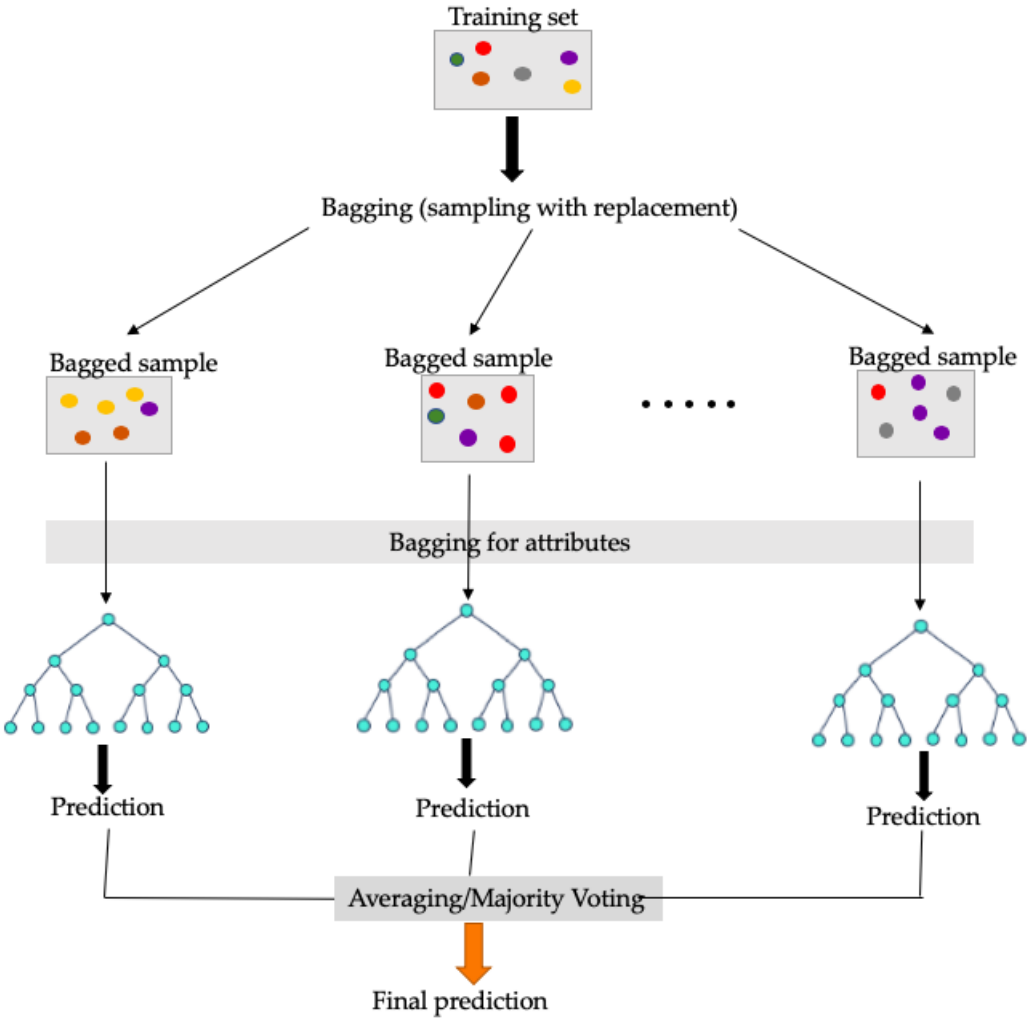

Figure 3.2. Simple random forest model [9].

The number of trees, the number of observations per leaf node, and the number of features used for splitting are several of the significant parameters set by users. The "number of trees" parameter indicates the number of trees to be constructed. Each tree is a different learner created using a different part of the training set and different feature list. The "number of observations" parameter specifies the minimum number of observations at a leaf node. If the resulting split node would be less than this value, a node cannot be split further. Larger values result in smaller trees and less computational time. Setting this value smaller results in larger trees and higher computational time. Additionally, keeping the node size small may cause over-fitting. The "number of features" parameter determines the number of features to be considered for splitting at each node.

3.4. Boosting Tree

Boosting is an ensemble method that seeks to improve prediction power by building a strong learner from a set of weak learners. The idea of this method is to train weak models sequentially, each attempts to compensate for the weakness of its predecessor. Observations that are misclassified or with large residual errors in the former iteration are re-weighted to upgrade the performance of the simple base-learner [105]. The ensemble output is the weighted sum:

$$\hat{Y}(x) = \sum_t w_t h_t(x) \tag{3.6}$$

where,

$$\begin{cases} h_t(x) & : \text{output of tree } t \\ w_t & : \text{weight of tree } t \text{ relative to its accuracy} \end{cases}$$

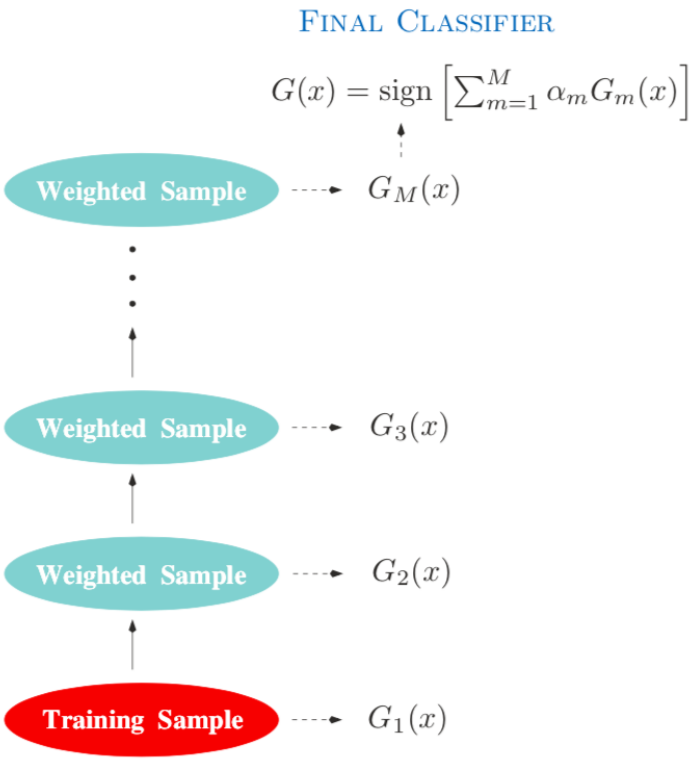

Figure 3.3. Schema of AdaBoost, which is the original version of boosting [10, 11].

Gradient Boosting is a method that combines boosting and gradient descent algorithm. Unlike AdaBoost, which adjusts the sample weights at each iteration, this strategy utilizes the gradient descent algorithm to minimize the errors in sequential models. The final prediction is obtained by summing up the prediction of all trees.

There are some important parameters to be adjusted such as interaction depth, number of trees, learning rate, etc.

- Interaction depth: It stands for the number of splits in each tree so that it controls the complexity of the boosted ensemble. It also specifies the maximum number of variables to be interacted during these splits. When the depth simply equals to one, each tree performs only one split and only one variable is included. When the depth is greater than one, more than one split is observed in each tree.
- The number of trees: It represents the number of trees in the forest. Each tree is constructed sequentially in order to model the residuals from the previous learner. More trees can provide better learning. However, depending on the magnitude of this parameter, the training process may slow down.
- Learning rate: This parameter stands for the contribution of each tree to the model. The small value of this parameter necessitates a very large number of trees to accomplish a good performance, whereas larger values result in overfitting and require less computational time.

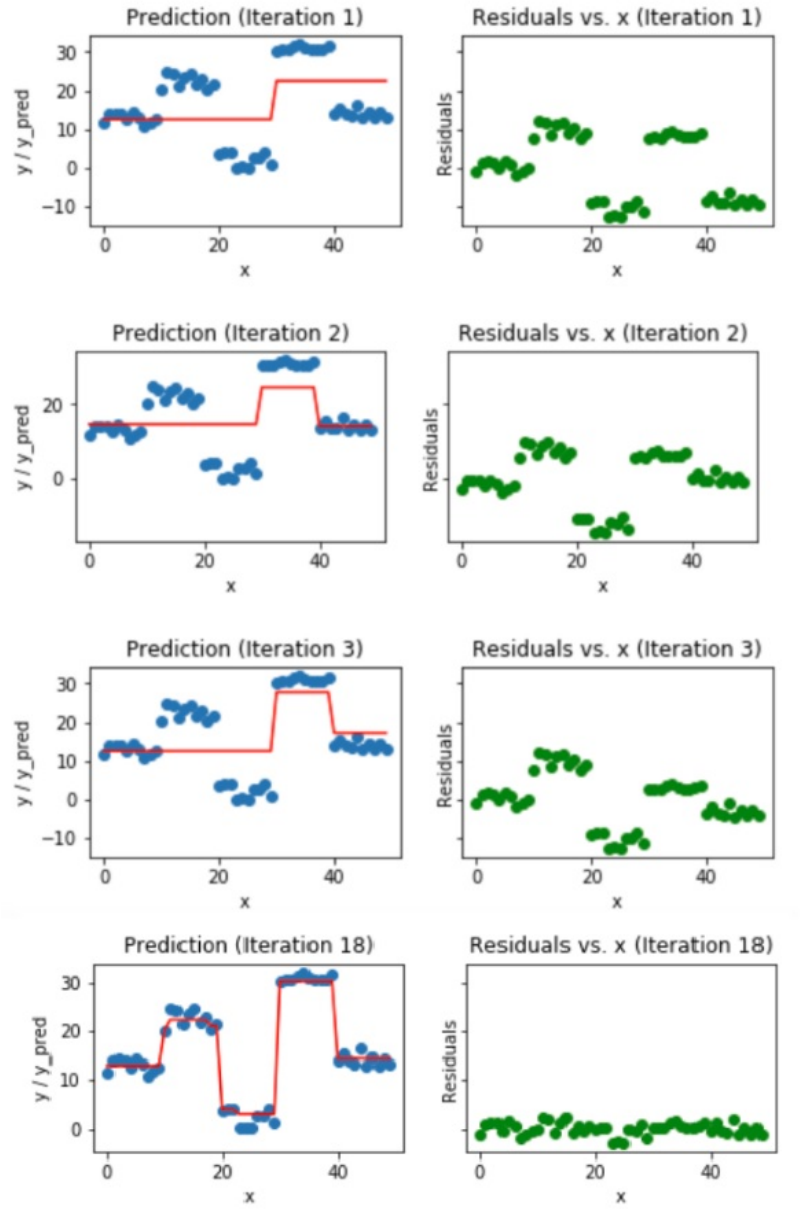

Figure 3.4. Gradient Boosting iterations [12].

XGBoost that stands for the Extreme Gradient Boosting is an enhanced version of the gradient boosting algorithm in terms of performance and speed. The goal of the XGBoost method is to minimize the following objective function:

$$O(x) = \sum_i l(\hat{y}_i, y_i) + \sum_i \Omega(f_t) \tag{3.7}$$

where $l(\hat{y}_i, y_i)$ represents the distance between the truth and the prediction of the i th

sample, and $\Omega(f_t)$ stands for the regularization function that penalizes the complexity of the t th tree to avoid over-fitting [106]. Since the standard gradient boosting does not provide regularization, XGBoost is known as "regularized boosting" [107].

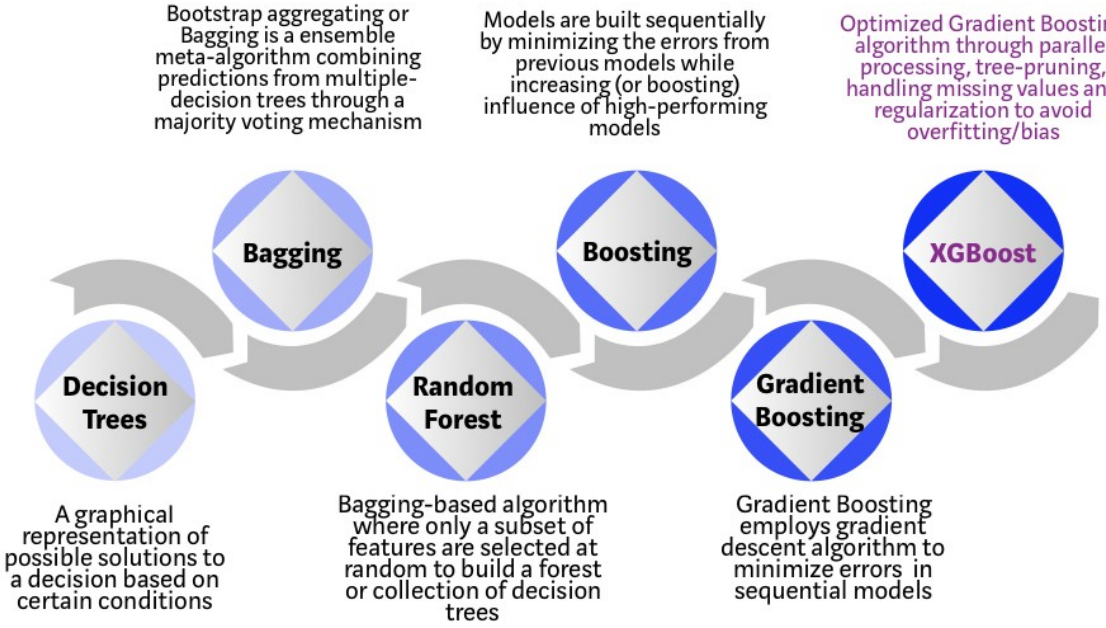

Figure 3.5. Evolution of XGBoost [13].

4. EXPERIMENTS

In this study, statistical software R has been used for data analysis and model implementation. For regression analysis, the "caret" package is used with methods backward and forward stepwise regressions. The packages *rpart* and *tree*, *randomForest*, *xgboost* are utilized for regression tree, random forest, and XGBoost methods, respectively.

4.1. Data

Between October 2013 and December 2016, the f-URS procedures for the treatment of urinary tract stones are retrospectively analyzed.

The variables used in the analysis are shown in Table 4.1.

Table 4.1. Variables considered for analysis.

Pre-operative variables	**Intra-operative variables**
Age	Type of anesthesia
Gender	Patient position
Weight(kg)	UAS length
Height(cm)	UAS thickness
ASA score	UAS placement level
Patient's complaint	Guidewire
Previous treatment	Semi-rigid URS
Stone history of patient	Stone opacity
Stone history of patient's family	Lithotripsy technique
Comorbidity	Residual stone size (if observed)
Additional urinary system disease	Laser probe thickness
Pre-operative hydronephrosis	Power (Laser setting)
Pre-operative urinary culture	Frequency (Laser setting)
Anticoagulant-Antiaggregant use	
Pre-operative antibiotic use	
Pre-operative DJ stent	
Pre-operative WBC	
Pre-operative hemoglobin	
Pre-operative radiological imaging technique	
Maximum hounsfield units	
Surgical site	
Stone location	
Number of stones	
Stone size (sum of long axes)	

4.1.1. Data Preprocessing

Data serves as the backbone for data mining and knowledge discovery. However, real-world data is generally not presented in a convenient format for data mining applications. Even if the data is stored in a database, it can be cumbersome to extract the right data from the database.

Data cleaning refers to the transformation of raw data into a useful and efficient format. In most data mining studies, the most time-consuming part is data cleaning and data organizing. Research shows that data preparation accounts for about 80% of the total time spent on the entire data mining process [108].

Observing missing values in a dataset is a commonly encountered problem in many real-world datasets. A dataset may contain missing values for various reasons, and this may lead to problems for in-depth analysis. Therefore, many alternative approaches for handling the missing data have been developed. One way to overcome the missing data problem is to discard the observations that contain missing data. However, this approach entails the risk of losing data points with important information. For this reason, it may be more beneficial to infer the missing values from the existing part of the data. This strategy is referred to as missing data imputation.

In the pre-processing stage, firstly, each observation is labeled by the instructions of a field expert. The instances with the residual stone observed at the end of the operation are labeled as "failure", while those with stone-free status as "success".

Three different approaches are applied to the missing data:

(i) List-wise Deletion

Elimination of observations containing one or more missing values turns the original dataset with 1166 observations into a dataset containing 135 failures and 360 successes. This dataset is referred to as Dataset 1 in the rest of the document.

(ii) Imputation with Multiple Imputation by Chained Equations (MICE)

Instead of imputing a single value for a missing entry, which is the case in the single imputation method, the multiple imputation (MI) method attempts to impute multiple values for the missing entry. Thus, it narrows the bias by providing several different options for the missing value. Several versions of the same data created for the missing values are combined to obtain the ultimate prediction. MICE, sometimes referred to as "sequential regression multiple imputation" [109], is a special version of the MI. In this approach, each variable containing the missing value(s) is treated as the dependent variable and regressed on some or all of the remaining variables. It is preferred for the cases where missing values are observed in several variables [110].

In this study, the "mice" package in R statistical software is utilized for imputation. The mice-imputed version of the raw dataset containing 1166 observations consists of 871 successes and 295 failures. This dataset is referred to as Dataset 2 in the rest of the document.

(iii) Step-by-step Imputation with KNN

In this approach, the observations with a missing value ratio greater than 30% are ignored. The resulting dataset is divided into two parts:

D_m: The set containing instances in which at least one of the variables is missing.

D_c: The set containing instances with complete variables.

Then, the following steps are carried out:

(a) For each observation s in D_m:

Divide the observation s into two parts as $s = [s_o, s_m]$, where s_m represents missing variables, and s_o indicates the complete ones.

(b) Select the instance with the least number of missing values from D_m.

(c) Calculate the distance between the s_o and all observations in D_c. During the calculation of distances, use only variables in the observation vectors D_c which are observed in vector s.

(d) Identify the five closest observations. If the missing attribute is continuous, replace the missing value with the mean of the attribute values found for the 5-nearest neighbors. For the categorical ones, implement the majority

voting method.

(e) Include the observation in the D_c.

(f) Carry out the steps (b)–(e) until no observations remain in D_m.

The KNN-imputed version of the raw dataset contains 1142 observations, consisting of 854 successes and 288 failures. This dataset is referred to as Dataset 3 in the rest of the document.

The methods for missing data imputation stated above are implemented in accordance with the need. Several descriptive statistics related to machine settings for each of the aforementioned datasets can be seen in Table 4.2.

Table 4.2. A few descriptive statistics for constructed datasets.

		Dataset 1 (List-wise deletion)	Dataset 2 (MICE)	Dataset 3 (KNN imputation)
Power	min	0.60	0.10	0.40
	max	3.00	3.00	3.00
	mean	1.59	1.49	1.52
	sd	0.64	0.64	0.60
Frequency	min	1.00	1.00	1.00
	max	20.00	20.00	20.00
	mean	9.81	11.21	10.35
	sd	2.67	4.57	3.62
# of observations		495	1166	1142

4.1.2. Model Implementation

For almost all methods, there exist parameters to be set to appropriate values. The number of parameters depends on the method. In this study, the default values are used as initial parameter values. Then, the parameter tuning procedure is performed by 10-fold cross-validation. Root Mean Square Error (RMSE) and Normalized Root

Mean Square Error (NRMSE) are used as performance measures.

$$RMSE = \sqrt{\frac{\sum_{i=1}^{n}(y_i - \hat{y}_i)^2}{n}} \tag{4.1}$$

$$NRMSE = \frac{RMSE}{y_{max} - y_{min}} \tag{4.2}$$

where $\hat{y}_i$ and y_i represent the predicted and observed value, respectively.

The missing data is first handled using the "mice" package. Thereafter, regression tree and linear regression methods are applied to Dataset 1 (list-wise deleted) and Dataset 2 (MICE-imputed). For the first stage only, the datasets are not separated into two subgroups as test set and training set. The results of these two methods are shown in Table 4.3.

Table 4.3. The RMSE and NRMSE values for each machine setting.

		Dataset 1 (List-wise deletion)		Dataset 2 (MICE)	
Method		RMSE	NRMSE	RMSE	NRMSE
Linear Regression	Success-Power	0.44	0.18	0.44	0.18
	Success-Frequency	1.92	0.10	2.93	0.15
	Failure-Power	0.55	0.23	0.46	0.19
	Failure-Frequency	2.51	0.13	3.14	0.17
Regression Tree	Success-Power	0.36	0.15	0.43	0.18
	Success-Frequency	1.75	0.09	2.77	0.15
	Failure-Power	0.35	0.15	0.38	0.16
	Failure-Frequency	1.97	0.10	2.71	0.14

As can be seen in Table 4.3, list-wise deleted dataset yields better results than the mice-imputed dataset in terms of RMSE values. For this reason, another imputation method called step-by-step KNN imputation method (mentioned above) is applied. The obtained results are listed in Table 4.4.

Table 4.4. The RMSE and NRMSE values for each machine setting.

		Dataset 1 (List-wise deletion)		Dataset 2 (MICE)		Dataset 3 (KNN)	
Method		RMSE	NRMSE	RMSE	NRMSE	RMSE	NRMSE
Linear Regression	Success-Power	0.44	0.18	0.44	0.18	0.44	0.18
	Success-Frequency	1.92	0.10	2.93	0.15	2.87	0.15
	Failure-Power	0.55	0.23	0.46	0.19	0.49	0.20
	Failure-Frequency	2.51	0.13	3.14	0.17	2.74	0.14
Regression Tree	Success-Power	0.36	0.15	0.43	0.18	0.42	0.18
	Success-Frequency	1.75	0.09	2.77	0.15	2.50	0.13
	Failure-Power	0.35	0.15	0.38	0.16	0.34	0.14
	Failure-Frequency	1.97	0.10	2.71	0.14	2.21	0.12

Although Dataset 3 yields better RMSE values compared to Dataset 2, it is still not as good as Dataset 1 which is obtained by the list-wise deletion method. Therefore, after this stage, Dataset 2 is excluded from the process. The study is continued using Dataset 1 and Dataset 3. In addition to linear regression and regression tree, XGBoost and random forest methods are applied to the available datasets.

For extreme gradient boosting method, model performances are tested by evaluating different values of max depth (interaction depth), learning rate (eta), and number of trees (nrounds), as can be seen in Table 4.5.

Table 4.5. Parameter values of the XGBoost method.

Parameters	**Values**
Interaction Depth (max_depth)	1, 3, 5, 7
Learning Rate (eta)	0.01, 0.02, 0.03, 0.05, 0.1, 0.2, 0.3
Number of Trees (nrounds)	100, 200, 300, 400, 500, 600, 700, 800, 900, 1000

For random forest, three parameters are estimated: number of trees, number of predictors for each tree, and node size. These parameters are searched over the values shown in Table 4.6.

Table 4.6. Parameter search for random forest.

Parameters	**Values**
Number of trees	200, 250, 300, 500
Number of predictors for each tree	10, 12, 15
Node size	3, 5, 10

As a result of the applied methods, the results shown in Table 4.7 are obtained.

Table 4.7. The RMSE and NRMSE values for each machine setting.

		Dataset 1 (List-wise deletion)		Dataset 3 (KNN)	
Method		RMSE	NRMSE	RMSE	NRMSE
Linear Regression	Success-Power	0.44	0.18	0.44	0.18
	Success-Frequency	1.92	0.10	2.87	0.15
	Faiure-Power	0.55	0.23	0.49	0.20
	Faiure-Frequency	2.51	0.13	2.74	0.14
Regression Tree	Success-Power	0.36	0.15	0.42	0.18
	Success-Frequency	1.75	0.09	2.50	0.13
	Faiure-Power	0.35	0.15	0.34	0.14
	Faiure-Frequency	1.97	0.10	2.21	0.12
Random Forest	Success-Power	0.17	0.07	0.17	0.07
	Success-Frequency	0.91	0.05	1.16	0.06
	Faiure-Power	0.21	0.09	0.21	0.09
	Faiure-Frequency	1.12	0.06	1.31	0.07
XGBoost	Success-Power	0.46	0.19	0.36	0.10
	Success-Frequency	0.21	0.01	5.24	0.28
	Faiure-Power	0.16	0.07	0.55	0.23
	Faiure-Frequency	0.89	0.05	1.75	0.09

4.1.3. Implementation of Established Models on Unseen Observations

The following steps are performed for both Dataset 1 and Dataset 3 in order to see the machine settings prediction power of the models and their differentiation capability.

(i) Divide Dataset 1 into two subgroups, “success” and “failure”.

(ii) Select five observations randomly from the subgroup “success” (“failure”), and exclude them from the subgroup. Apply linear regression, regression tree, random forest, and XGBoost methods using data remaining in this subgroup.

(iii) Apply regression tree, random forest, and XGBoost methods using data from the

other subgroup "failure" ("success").

(iv) Estimate settings for five observations that have been removed from the subgroup "success" ("failure") using models constructed on successful (failed) observations.

(v) Estimate settings for five observations that have been removed from the subgroup "success" ("failure") using models constructed on failed (successful) observations.

(vi) Compare the results.

As can be seen in Figures 4.1, 4.2, 4.3, and 4.4, there is not a significant difference between predictions of models trained on the "success" cases and models trained on the "failure" cases. In other words, the differentiation capability of the models is not as strong as expected.

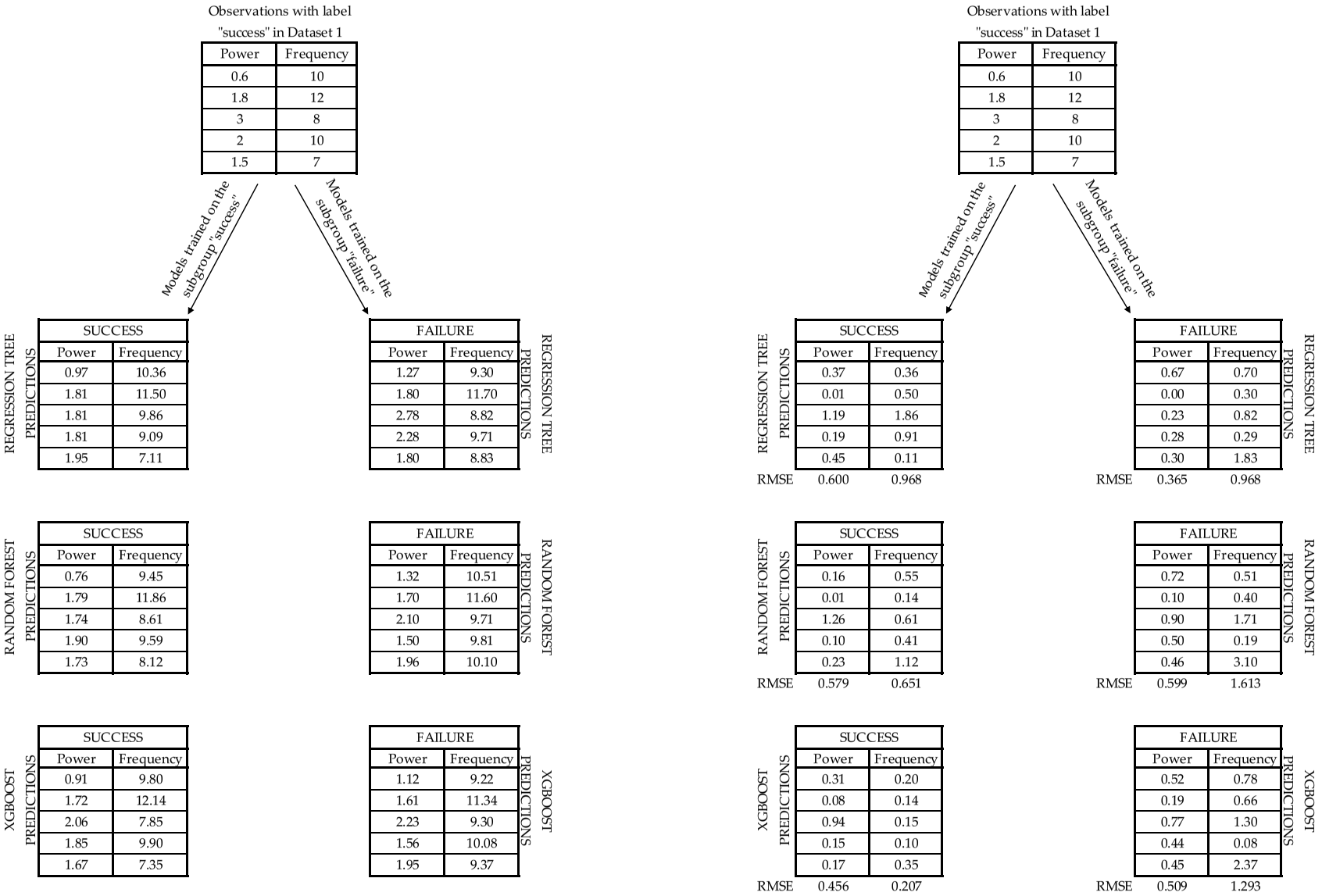

Figure 4.1. Predictions of the models trained on “success” subset of Dataset 1 for “success” instances from Dataset 1.

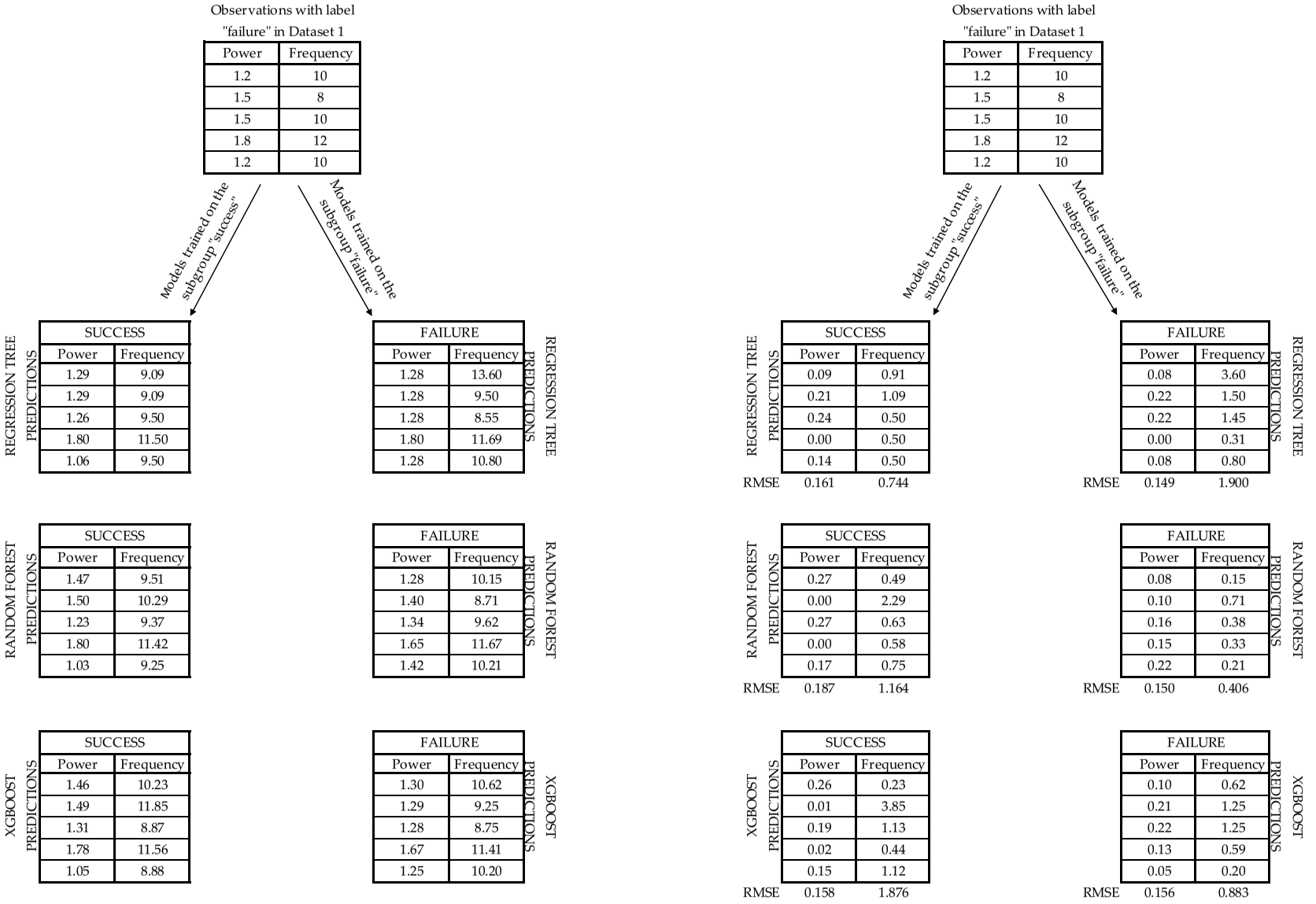

Figure 4.2. Predictions of the models trained on “failure” subset of Dataset 1 for “failure” instances from Dataset 1.

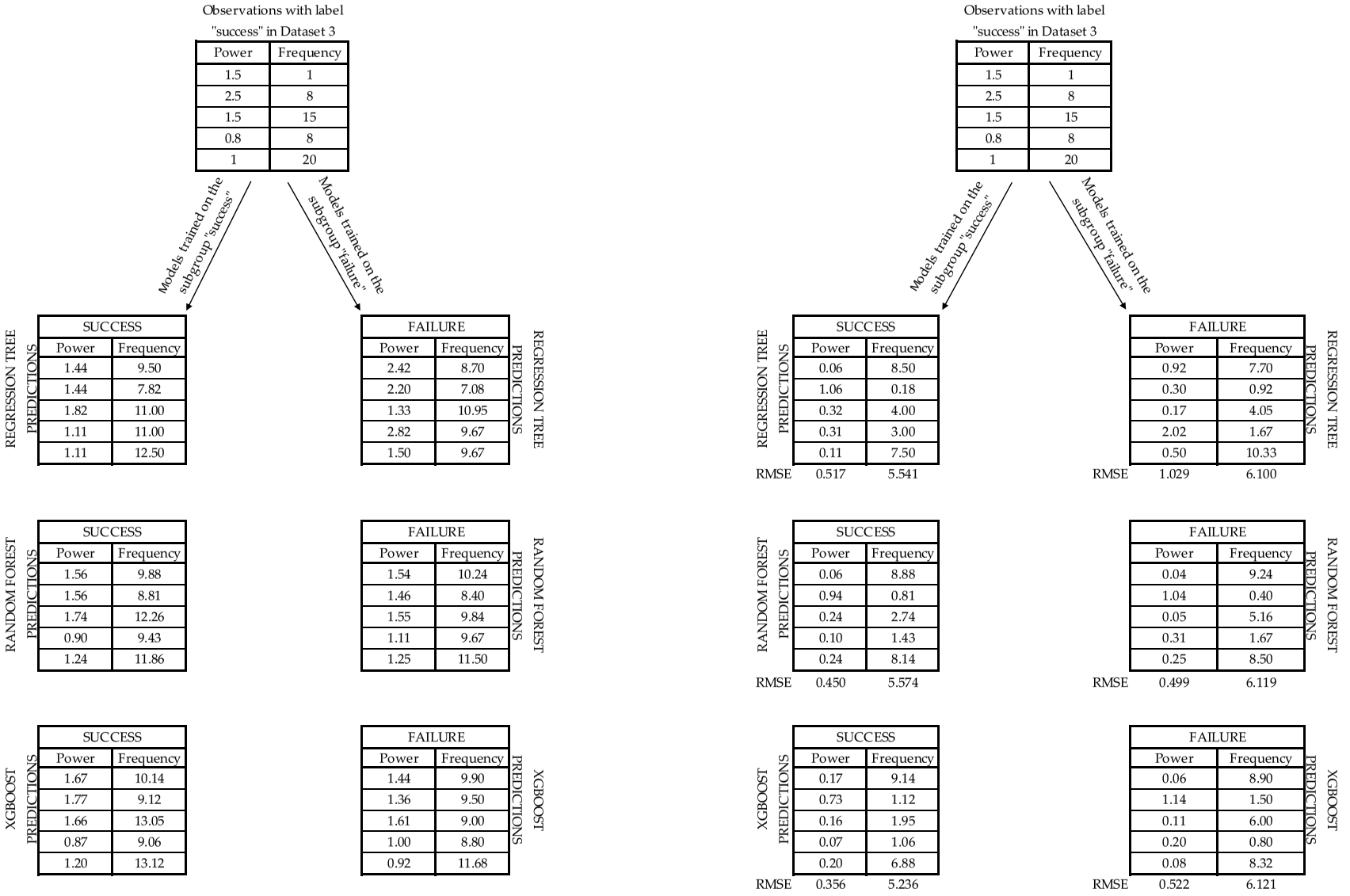

Figure 4.3. Predictions of the models trained on “success” subset of Dataset 3 for “success” instances from Dataset 3.

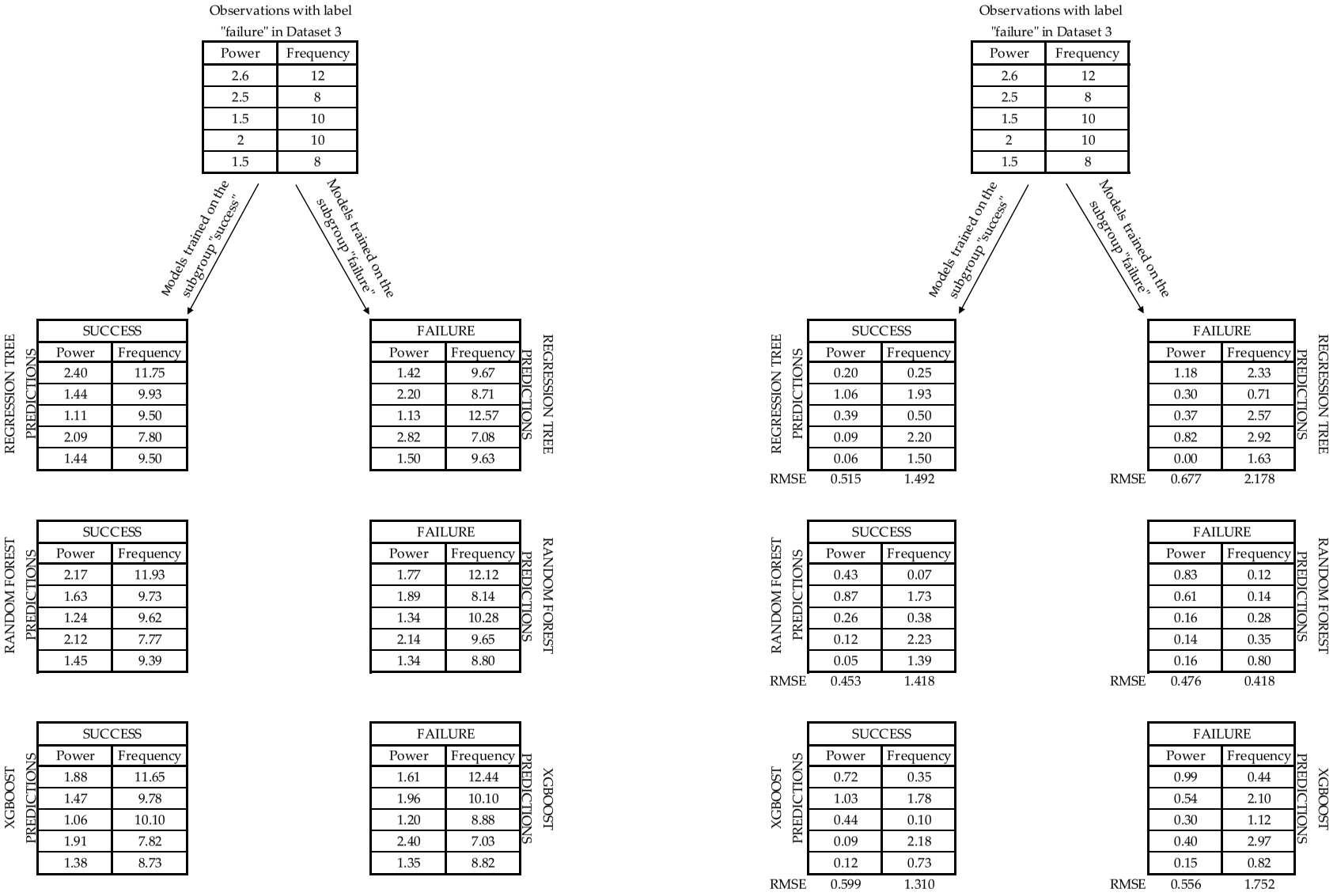

Figure 4.4. Predictions of the models trained on “failure” subset of Dataset 3 for “failure” instances from Dataset 3.

There are two potential reasons why the analysis does not yield satisfactory results. The first and more important one is that the raw dataset contains a significant amount of missing data. The dataset obtained as a result of removing incomplete observations contains 135 "failure" and 405 "success" observations. The obtained dataset, called Dataset 1, contains relatively few data for data mining problems. Therefore, it is possible that the desired degree of learning from the data cannot be achieved. The other possible reason is that the step-by-step imputation method with KNN is problematic. This can explain why the models trained on Dataset 3 do not provide the expected prediction success.

4.2. Synthetic Data Generation

In order to overcome the obstacles stated in the previous section, synthetic data generation is considered as an alternative. In the process of synthetic data generation, a package called *"synthpop"* is utilized. This package enables users to create synthetic versions of an original dataset. In this tool, variables are synthesized one-by-one. Synthetic values are generated by taking the advantage of conditional distributions fitted to the original data using CART (Classification and Regression Trees) as default. The basic steps followed in the synthpop package are illustrated in Figure 4.5.

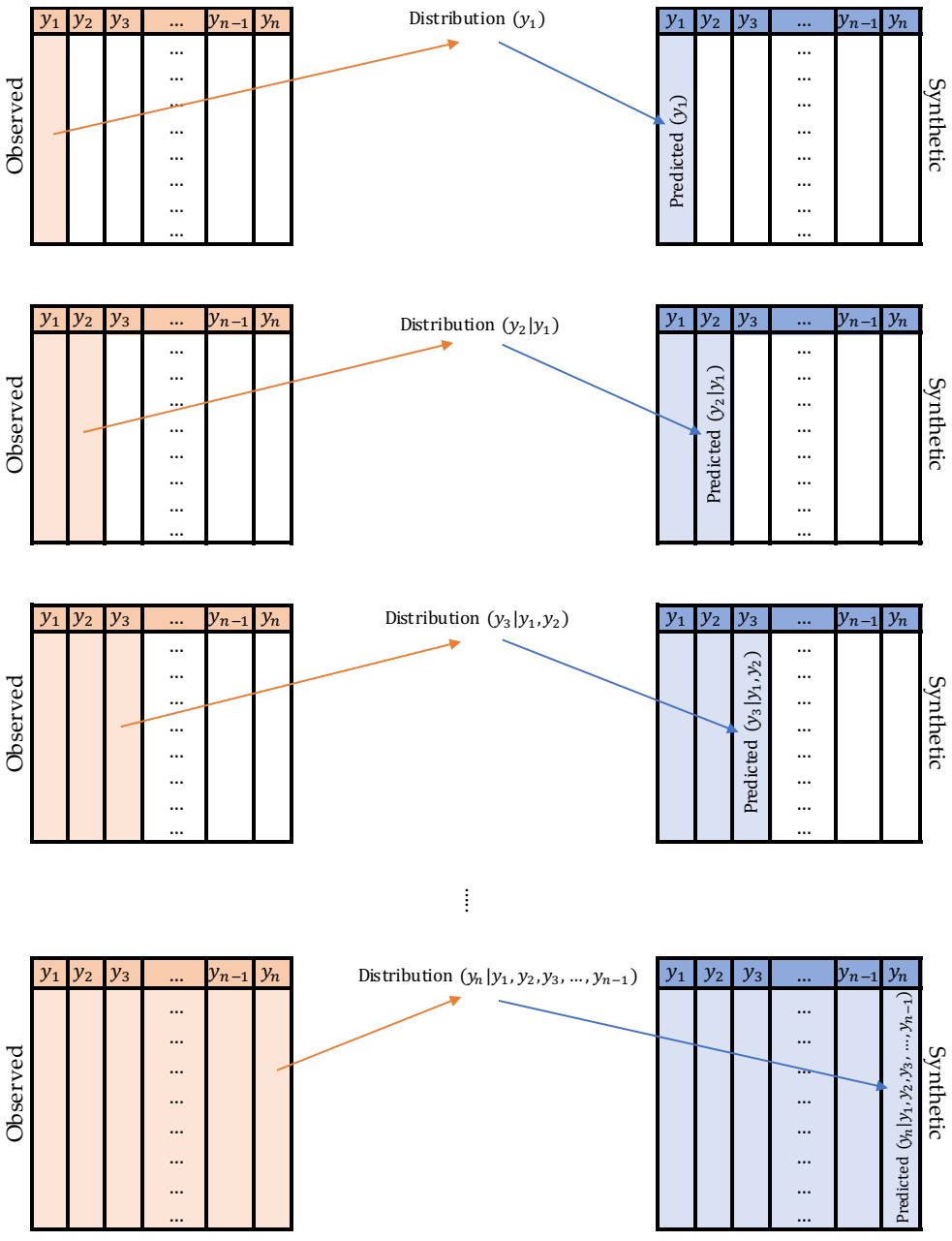

Figure 4.5. Basic synthpop process [14].

The *"utility.gen"* function in the package allows users to compare generated dataset with the original dataset using propensity scores. Propensity scores represent the probabilities of group memberships. To use this score as a quality indicator, it is needed to model group membership between the original and the synthetic data to obtain a prediction of differentiation. Small differentiation relates to high distributional similarity between the original and synthetic data [15]. The propensity score approach

proceeds as described in Figure 4.6. The method can be assumed as a classification problem where the expected result is poor classification.

Algorithm 1 General Utility Statistic Based on Propensity Score Mean-Squared Error

1: stack the original n_1 rows, Y_{real} and the n_2 rows of masked data Y_{syn} to create the $N = n_1 + n_2$ rows of Y_{comb}
2: add an indicator variable, I, to Y_{comb} s.t. $I = \{1 : y_i \in Y_{syn}\}$
3: fit a model to predict I using predictors Z_{comb} calculated from Y_{comb}.
4: predict propensity scores, $\hat{p}_i$, for each row of Z_{comb}
5: obtain the utility statistic from $\frac{1}{N}\Sigma_{i=1}^{N}(\hat{p}_i - c)^2$ where $c = n_2/N$ is the proportion of records in Y_{comb} from Y_{syn}

Figure 4.6. The propensity score method [15].

The mean squared difference between propensity scores $\hat{p}_i$ (calculated for each row of the dataset which is the combination of the original data and the synthetic data) and the actual proportion of the synthetic data c yields a utility statistic which is referred to as propensity score mean-squared-error (pMSE). The pMSE value near zero indicates a small differentiation between the original data and the synthesized data, where the value of zero is obtained in the state of the identicalness of the original data and the synthetic data [15].

Another function offered in the package is *"compare"*, which compares synthesized dataset with the original dataset using the frequency distribution of each variable. The comparison is provided in both tabular and graphic form.

Since Dataset 1 yields the lowest RMSE values compared to the Dataset 2 and Dataset 3 (as seen in Tables 4.4 and 4.7), a synthetic dataset is decided to be generated based on Dataset 1. To do this, firstly, observations in Dataset 1 are divided into two subgroups according to their labels "success" or "failure". Based on these two subgroups, two synthetic datasets are generated: one for the success cases, the other for the failures as illustrated in Figure 4.7.

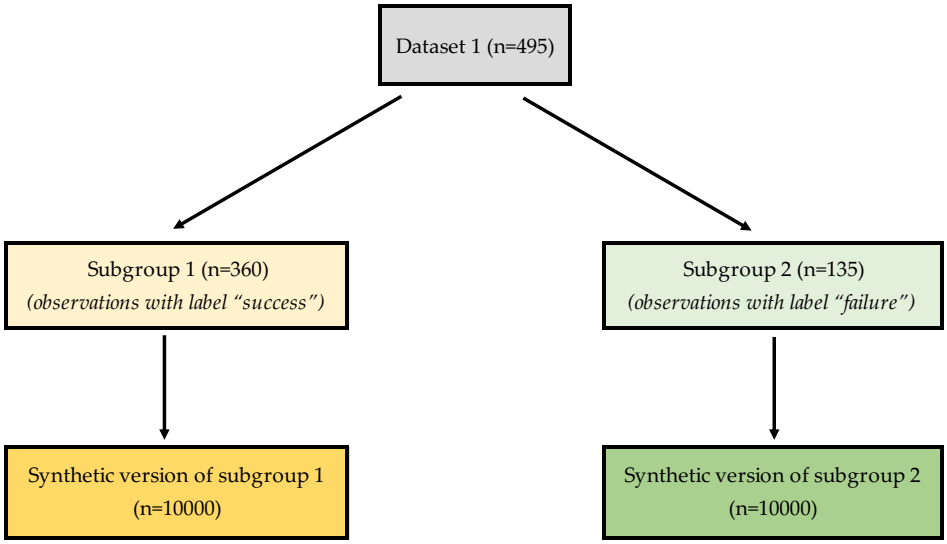

Figure 4.7. Synthetic data generation.

Comparison of synthetic and original datasets for each "success" and "failure" observations are shown in Figure 4.8 and 4.9, respectively. As the figures suggest, synthetic data and original data follow a similar distribution pattern in terms of variable frequency.

Another function offered in the package is *"utility.gen"*, which enables users to assess the quality of the synthetic datasets. When this function is applied to each synthetic dataset, pMSE values are found to be 0.03 and 0.01 with p-values < 0.0001, respectively. These results indicate insignificant difference between the original and synthesized dataset.

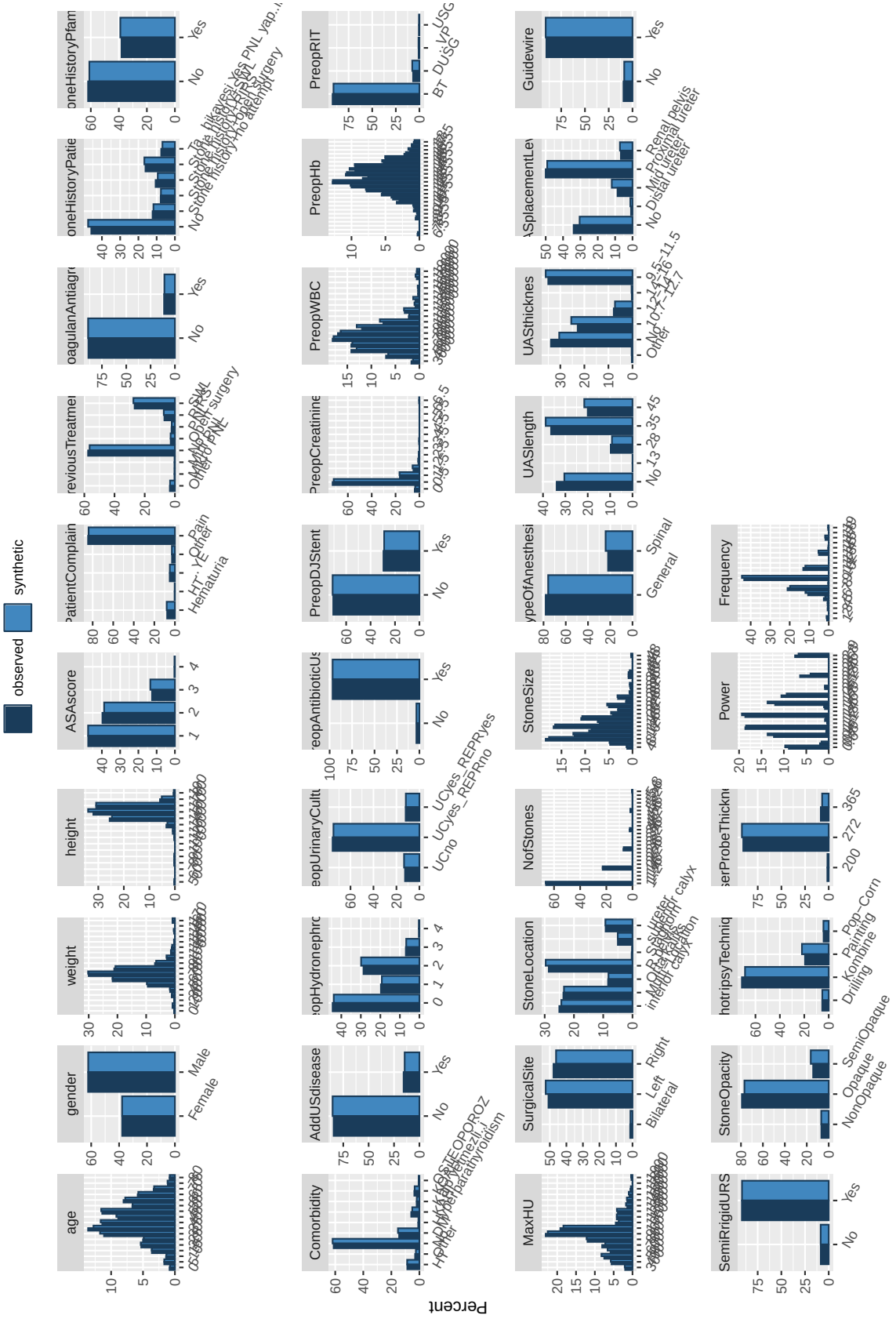

Figure 4.8. Comparison of synthetic and original datasets for "success" cases.

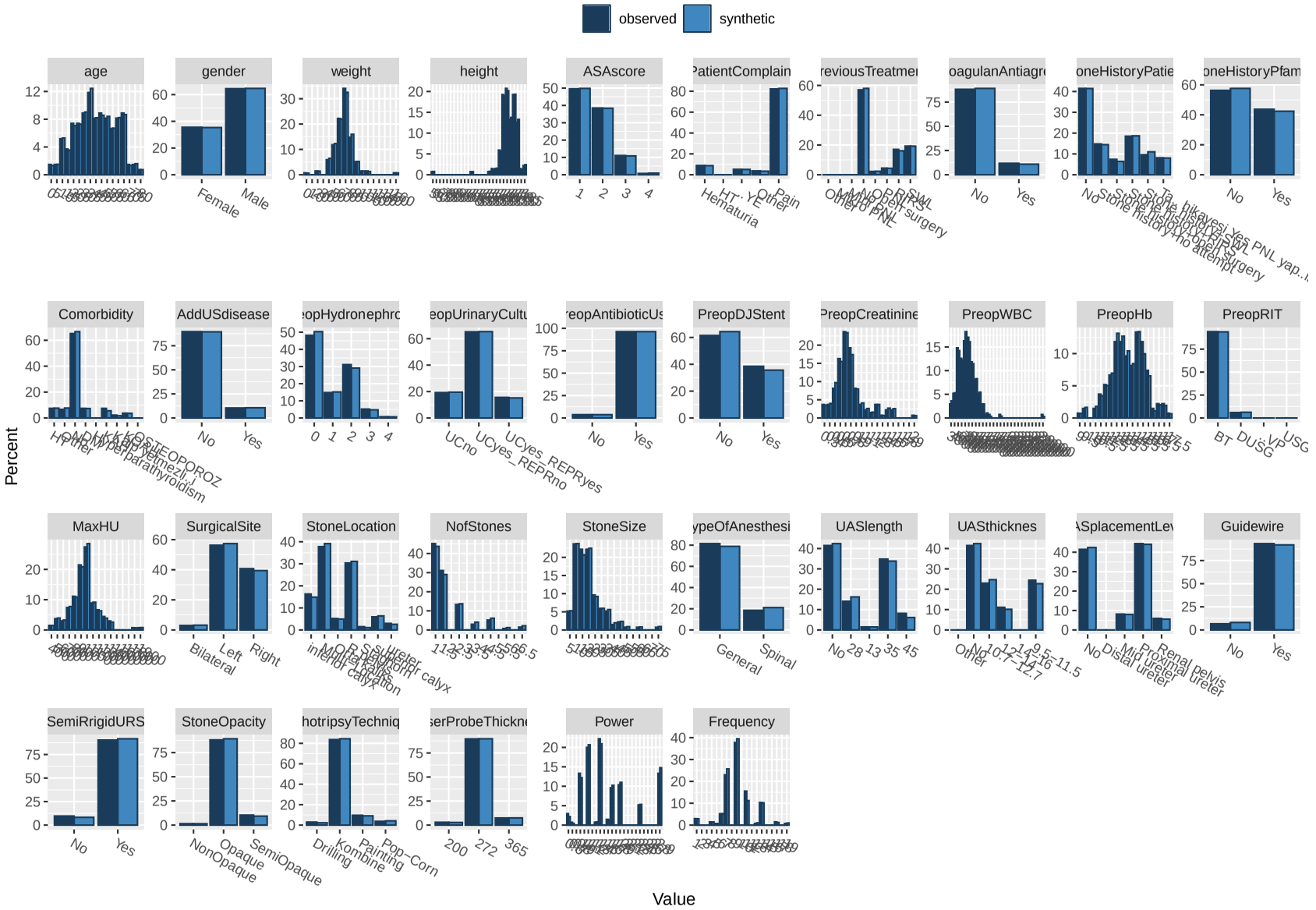

Figure 4.9. Comparison of synthetic and original datasets for “failure” cases.

4.2.1. Model Implementation on Synthetic Dataset

In this section, the previous methods are applied for synthesized datasets. The models trained on synthetic datasets are tested on their original versions.

For extreme gradient boosting method, model performances are tested by evaluating different values of max depth (interaction depth), learning rate (eta), and number of trees (nrounds) as can be seen in Table 4.8).

Table 4.8. Parameter values of XGBoost method.

Parameters	**Values**
Interaction Depth (max_depth)	1, 3, 5, 7
Learning Rate (eta)	0.01, 0.02, 0.03, 0.05, 0.1, 0.2, 0.3
Number of Trees (nrounds)	100, 200, 300, 400, 500, 600, 700, 800, 900, 1000

For random forest, three parameters are estimated: number of trees, number of predictors for each tree, and node size. These parameters are searched over the values shown in Table 4.9.

Table 4.9. Parameter search for random forest.

Parameters	**Values**
Number of trees	200, 250, 300, 500
Number of predictors for each tree	10, 12, 15
Node size	3, 5, 10

After the determination of the best parameter combinations, the obtained models are tested on the original datasets. RMSE and NRMSE are used as performance measures.

$$RMSE = \sqrt{\frac{\sum_{i=1}^{n}(y_i - \hat{y}_i)^2}{n}} \tag{4.3}$$

$$NRMSE = \frac{RMSE}{y_{max} - y_{min}} \tag{4.4}$$

where $\hat{y}_i$ and y_i represent the predicted and observed value, respectively.

Tables 4.10 and 4.11 summarize the results of models constructed on synthetic datasets for the prediction of *"original success"* and *"original failure"* datasets, respectively. The results indicate that the random forest method yields better results compared to the other methods. Furthermore, models trained on success cases and models trained on failure cases provide different estimates for machine settings.

Table 4.10. RMSE values of estimates for original datasets of models built on synthetic datasets.

	Success-Power		Success-Frequency		Failure-Power		Failure-Frequency	
Models trained on synthetic	Success	Failure	Success	Failure	Failure	Success	Failure	Success
Random Forest	0.3296	0.6021	1.7759	2.6674	0.3640	0.5660	2.1412	2.9998
Regression Tree	0.4196	0.6403	1.9218	2.6612	0.3946	0.5526	2.1935	3.0523
XGBoost	0.3637	0.5819	1.9537	2.6380	0.3638	0.5070	2.1733	2.9073
Linear Regression	0.5060	0.8702	2.4201	2.6246	0.5088	0.5682	2.9477	3.0052

Table 4.11. NRMSE values of estimates for original datasets of models built on synthetic datasets.

	Success-Power		Success-Frequency		Failure-Power		Failure-Frequency	
Models trained on synthetic	Success	Failure	Success	Failure	Failure	Success	Failure	Success
Random Forest	0.1373	0.2509	0.0935	0.1404	0.1517	0.2358	0.1127	0.1579
Regression Tree	0.1748	0.2668	0.1011	0.1401	0.1644	0.2302	0.1154	0.1606
XGBoost	0.1515	0.2425	0.1028	0.1388	0.1516	0.2112	0.1144	0.1530
Linear Regression	0.2108	0.3626	0.1274	0.1381	0.2120	0.2367	0.1551	0.1582

Table 4.12. RMSE and NRMSE values of estimates for original *"success"* dataset of models built on synthetic dataset.

	Success-Power				Success-Frequency			
	Predictions of models trained on "syn.success"		Predictions of models trained on "syn.failure"		Predictions of models trained on "syn.success"		Predictions of models trained on "syn.failure"	
	RMSE	NRMSE	RMSE	NRMSE	RMSE	NRMSE	RMSE	NRMSE
Random Forest	0.3296	0.1373	0.6021	0.2509	1.7759	0.0935	2.6674	0.1404
Regression Tree	0.4196	0.1748	0.6403	0.2668	1.9218	0.1011	2.6612	0.1401
XGBoost	0.3637	0.1515	0.5819	0.2425	1.9537	0.1028	2.6380	0.1388
Linear Regression	0.5060	0.2108	0.8702	0.3626	2.4201	0.1274	2.6246	0.1381

Table 4.13. RMSE and NRMSE values of estimates for original *"failure"* dataset of models built on synthetic dataset.

	Failure-Power				Failure-Frequency			
	Predictions of models trained on "syn.failure"		Predictions of models trained on "syn.success"		Predictions of models trained on "syn.failure"		Predictions of models trained on "syn.success"	
	RMSE	NRMSE	RMSE	NRMSE	RMSE	NRMSE	RMSE	NRMSE
Random Forest	0.3640	0.1517	0.5660	0.2358	2.1412	0.1127	2.9998	0.1579
Regression Tree	0.3946	0.1644	0.5526	0.2302	2.1935	0.1154	3.0523	0.1606
XGBoost	0.3638	0.1516	0.5070	0.2112	2.1733	0.1144	2.9073	0.1530
Linear Regression	0.5088	0.2120	0.5682	0.2367	2.9477	0.1551	3.0052	0.1582

5. CONCLUSION

The main motivation of this study is to determine patient-based machine settings for successful completion of an operation using the Retrograde Intrarenal Surgery (RIRS) method. In order for an operation to be considered as successful, a stone-free status must be observed at the end of the operation. Based on this definition, observations in the dataset provided by the urology department of İstanbul Medipol University Hospital are labeled by the guidance of a field expert. Following this labeling process, the dataset is divided into two subgroups: observations with the label *"success"*, and observations with the label *"failure"*.

At the beginning of the study, it is aimed to establish models using various data mining methods on these two groups for machine setting estimations. Models trained on successful cases and on failed cases are separately expected to give different estimates for machine settings since the datasets on which they are trained are different. However, the expected results are not obtained. Two things have been considered as potential reasons for the failure to achieve the expected goal. The most important of these is that the raw dataset contains a significant amount of missing entries. Thus, the desired degree of learning from the data could not be achieved. The other possible reason is the failure of imputation methods.

As a different approach, it is decided to produce synthetic data based on the original dataset. Models trained on synthetic data are tested on the original data. The models that are trained on synthetic data yield better estimates. Furthermore, the expectation of observing a difference between predictions of models constructed on "success" cases and "failure" cases is met.

The dataset utilized during the study consists of information about a small number of patients. Besides, the dataset contains a significant amount of missing data. Better results can be achieved with a more comprehensive dataset for a larger number of patients.

REFERENCES

1. Erdoğru, T., *Fleksibl Endoskopik (Üreteroskopik) Cerrahi Nedir?*, 2018, shorturl.at/ouIX6, accessed March 23, 2020.

2. *Ureteral Access Sheath, For Hospital*, 2020, https://www.indiamart.com/proddetail/ureteral-access-sheath-13777287612.html, accessed March 24, 2020.

3. *Plasti-med*, https://www.plasti-med.com/tr/sifir-uclu-nitinol-basket.html, accessed June 29, 2020.

4. *Urology Associates*, 2020, https://www.urology.co.nz/info/removing-your-stent, accessed March 26, 2020.

5. Doizi, S. and O. Traxer, "Flexible ureteroscopy: technique, tips and tricks", *Urolithiasis*, Vol. 46, No. 1, pp. 47–58, 2017, https://doi.org/10.1007/s00240-017-1030-x.

6. Ray, S., *Quick Introduction to Boosting Algorithms in Machine Learning*, 2015, https://uroweb.org, accessed March 20, 2020.

7. Kronenberg, P. and O. Traxer, "In vitrofragmentation efficiency of holmium: yttrium-aluminum-garnet (YAG) laser lithotripsy - a comprehensive study encompassing different frequencies, pulse energies, total power levels and laser fibre diameters", *BJU International*, Vol. 114, No. 2, pp. 261–267, 2014, https://doi.org/10.1111/bju.12567.

8. Drakos, G., *Decision Tree Regressor explained in depth*, 2019, https://gdcoder.com/decision-tree-regressor-explained-in-depth/, accessed June 29, 2020.

9. *Seeing the Forest for the Trees: An Introduction to Random Forest*, 2019, shorturl.at/knIUV, accessed February 15, 2020.

10. Wasserman, L., *All of Statistics*, Springer New York, 2004, https://doi.org/10.1007/978-0-387-21736-9.

11. Hastie, T., R. Tibshirani and J. Friedman, *The Elements of Statistical Learning*, Springer New York, 2009, https://doi.org/10.1007/978-0-387-84858-7.

12. *Gradyan Artırma(Gradient Boosting)*, 2018, https://devhunteryz.wordpress.com/2018/07/11/gradyan-arttirmagradient-boosting/, accessed June 9, 2020.

13. Morde, V., *XGBoost Algorithm: Long May She Reign!*, 2019, https://towardsdatascience.com/https-medium-com-vishalmorde-xgboost-algorithm-long-she-may-rein-edd9f99be63d, accessed February 2, 2020.

14. Raab, G., *Widening access to confidential data with the synthpop package*, 2017, https://www.closer.ac.uk/wp-content/uploads/Widening-access-to-confidential-data-with-the-synthpop-package-Gillian-Raab.pdf, accessed June 6, 2020.

15. Snoke, J., G. M. Raab, B. Nowok, C. Dibben and A. Slavkovic, "General and specific utility measures for synthetic data", *Journal of the Royal Statistical Society: Series A (Statistics in Society)*, Vol. 181, No. 3, pp. 663–688, 2018, https://doi.org/10.1111/rssa.12358.

16. Kazemi, Y. and S. A. Mirroshandel, "A novel method for predicting kidney stone type using ensemble learning", *Artificial Intelligence in Medicine*, Vol. 84, pp. 117–126, 2018, https://doi.org/10.1016/j.artmed.2017.12.001.

17. Chauhan, C. K., M. J. Joshi and A. D. B. Vaidya, "Growth inhibition of Struvite crystals in the presence of herbal extract Commiphora wightii", *Journal*

of Materials Science: Materials in Medicine, Vol. 20, No. S1, pp. 85–92, 2008, https://doi.org/10.1007/s10856-008-3489-z.

18. Scales, C. D., A. C. Smith, J. M. Hanley and C. S. Saigal, "Prevalence of Kidney Stones in the United States", *European Urology*, Vol. 62, No. 1, pp. 160–165, 2012, https://doi.org/10.1016/j.eururo.2012.03.052.

19. Edvardsson, V. O., O. S. Indridason, G. Haraldsson, O. Kjartansson and R. Palsson, "Temporal trends in the incidence of kidney stone disease", *Kidney International*, Vol. 83, No. 1, pp. 146–152, 2013, https://doi.org/10.1038/ki.2012.320.

20. Joseph, K., B. Parekh and M. Joshi, "Inhibition of growth of urinary type calcium hydrogen phosphate dihydrate crystals by tartaric acid and tamarind", *Current Science*, Vol. 88, pp. 1232–1238, 2005.

21. Cone, E. B., G. Pareek, M. Ursiny and B. Eisner, "Cost-effectiveness comparison of ureteral calculi treated with ureteroscopic laser lithotripsy versus shockwave lithotripsy", *World Journal of Urology*, Vol. 35, No. 1, pp. 161–166, 2016, https://doi.org/10.1007/s00345-016-1842-2.

22. Nouri, A. and M. Hassali, "Assessment of kidney stone disease prevalence in a teaching hospital", *African Journal of Urology*, Vol. 24, No. 3, pp. 180–185, 2018, https://doi.org/10.1016/j.afju.2018.05.003.

23. Hassan, M., A. R. El-Nahas, K. Z. Sheir, N. A. El-Tabey, A. M. El-Assmy, A. M. Elshal and A. A. Shokeir, "Percutaneous nephrolithotomy vs. extracorporeal shockwave lithotripsy for treating a 20–30 mm single renal pelvic stone", *Arab Journal of Urology*, Vol. 13, No. 3, pp. 212–216, 2015, https://doi.org/10.1016/j.aju.2015.04.002.

24. Goldberg, H., D. Golomb, Y. Shtabholtz, S. Tapiero, G. Creiderman, A. Shariv, J. Baniel and D. Lifhshitz, "The "old" 15 mm renal stone size limit for RIRS

remains a clinically significant threshold size", *World Journal of Urology*, Vol. 35, No. 12, pp. 1947–1954, 2017, https://doi.org/10.1007/s00345-017-2075-8.

25. Cleynenbreugel, B. V., O. Kilic and M. Akand, "Retrograde intrarenal surgery for renal stones - Part 1", *Türk Üroloji Dergisi/Turkish Journal of Urology*, Vol. 43, No. 2, pp. 112–121, 2017, https://doi.org/10.5152/tud.2017.03708.

26. Yaycioglu, O., S. Guvel, F. Kilinc, T. Egilmez and H. Ozkardes, "Results with 7.5F versus 10F rigid ureteroscopes in treatment of ureteral calculi", *Urology*, Vol. 64, No. 4, pp. 643–646, 2004, https://doi.org/10.1016/j.urology.2004.05.050.

27. Marshall, V. F., "Fiber Optics in Urology", *Journal of Urology*, Vol. 91, No. 1, pp. 110–114, 1964, https://doi.org/10.1016/s0022-5347(17)64066-7.

28. Herrero, M. R.-M., S. Doizi, E. X. Keller, V. D. Coninck and O. Traxer, "Retrograde intrarenal surgery: An expanding role in treatment of urolithiasis", *Asian Journal of Urology*, Vol. 5, No. 4, pp. 264–273, 2018, https://doi.org/10.1016/j.ajur.2018.06.005.

29. Black, K. M., A. H. Aldoukhi and K. R. Ghani, "A Users Guide to Holmium Laser Lithotripsy Settings in the Modern Era", *Frontiers in Surgery*, Vol. 6, p. 48, 2019, https://doi.org/10.3389/fsurg.2019.00048.

30. Alelign, T. and B. Petros, "Kidney Stone Disease: An Update on Current Concepts", *Advances in Urology*, Vol. 2018, pp. 1–12, 2018, https://doi.org/10.1155/2018/3068365.

31. Barbas, C., A. Garcia, L. Saavedra and M. Muros, "Urinary analysis of nephrolithiasis markers", *Journal of Chromatography B*, Vol. 781, No. 1-2, pp. 433–455, 2002, https://doi.org/10.1016/s1570-0232(02)00557-3.

32. "Scientific Program of 34th World Congress of Endourology & SWL Program Book and Abstracts", *Journal of Endourology*, Vol. 30, No. S2, pp. P1–A464,

2016, https://doi.org/10.1089/end.2016.29020.abstracts.

33. Alelign, T. and B. Petros, "Kidney Stone Disease: An Update on Current Concepts", *Advances in Urology*, Vol. 2018, pp. 1–12, 2018, https://doi.org/10.1155/2018/3068365.

34. Fakheri, R. J. and D. S. Goldfarb, "Association of nephrolithiasis prevalence rates with ambient temperature in the United States: a re-analysis", *Kidney International*, Vol. 76, No. 7, p. 798, 2009, https://doi.org/10.1038/ki.2009.274.

35. Moe, O. W., "Kidney stones: pathophysiology and medical management", *The Lancet*, Vol. 367, No. 9507, pp. 333–344, 2006, https://doi.org/10.1016/s0140-6736(06)68071-9.

36. Ceylan, C., S. Dogan, G. Saydam, M. Z. Kocak and O. G. Doluoglu, "Evaluation of the Process of Recycling and Renal Parenchymal Injury after ESWL with Metabolites Excreted in the Urine", *Renal Failure*, Vol. 35, No. 4, pp. 466–471, 2013, https://doi.org/10.3109/0886022x.2013.766574.

37. Antonov, I., "Some Theoretical Considerations About Possibility of Limitation of ESWL Procedure Injures", *Trakia Journal of Sciences*, Vol. 8, pp. 84 – 91, 2010.

38. Lin, M.-F., "The accessibility, efficiency, and cost analysis of flexible ureteroscopy with a holmium:YAG laser in treating large-sized renal calculi", *Urological Science*, Vol. 23, No. 3, pp. 67–69, 2012, https://doi.org/10.1016/j.urols.2012.07.004.

39. Eisner, B. H. and N. Nimmagadda, "Shock-wave Lithotripsy of Renal Calculi", *Smiths Textbook of Endourology*, pp. 731–744, John Wiley & Sons Ltd, 2018, https://doi.org/10.1002/9781119245193.ch60.

40. Abdel-Khalek, M., K. Z. Sheir, E. Elsobky, S. Showkey and M. Kenawy, "Prognos-

tic factors for extracorporeal shock-wave lithotripsy of ureteric stones: A multivariate analysis study", *Scandinavian Journal of Urology and Nephrology*, Vol. 37, No. 5, pp. 413–418, 2003, https://doi.org/10.1080/00365590310006255.

41. Choo, M. S., S. Uhmn, J. K. Kim, J. H. Han, D.-H. Kim, J. Kim and S. H. Lee, "A Prediction Model Using Machine Learning Algorithm for Assessing Stone-Free Status after Single Session Shock Wave Lithotripsy to Treat Ureteral Stones", *Journal of Urology*, Vol. 200, No. 6, pp. 1371–1377, 2018, https://doi.org/10.1016/j.juro.2018.06.077.

42. Charig, C. R., D. R. Webb, S. R. Payne and J. E. Wickham, "Comparison of treatment of renal calculi by open surgery, percutaneous nephrolithotomy, and extracorporeal shockwave lithotripsy.", *BMJ*, Vol. 292, No. 6524, pp. 879–882, 1986, https://doi.org/10.1136/bmj.292.6524.879.

43. Çitamak, B., H. Dogan, T. Ceylan, B. Hazir, C. Bilen, A. Sahin and S. Tekgül, "A new simple scoring system for prediction of success and complication rates in pediatric percutaneous nephrolithotomy: stone-kidney size score", *Journal of Pediatric Urology*, Vol. 15, No. 1, pp. 67.e1–67.e6, 2019, https://doi.org/10.1016/j.jpurol.2018.09.019.

44. Ganpule, A. P., M. Vijayakumar, A. Malpani and M. R. Desai, "Percutaneous nephrolithotomy (PCNL) a critical review", *International Journal of Surgery*, Vol. 36, pp. 660–664, 2016, https://doi.org/10.1016/j.ijsu.2016.11.028.

45. Kyriazis, I., V. Panagopoulos, P. Kallidonis, M. Özsoy, M. Vasilas and E. Liatsikos, "Complications in percutaneous nephrolithotomy", *World Journal of Urology*, Vol. 33, No. 8, pp. 1069–1077, 2014, https://doi.org/10.1007/s00345-014-1400-8.

46. Jackman, S. V., S. G. Docimo, J. A. Cadeddu, J. T. Bishoff, L. R. Kavoussi and T. W. Jarrett, "The "mini-perc" technique: a less invasive alternative to percutaneous nephrolithotomy", *World Journal of Urology*, Vol. 16, No. 6, pp.

371–374, 1998, https://doi.org/10.1007/s003450050083.

47. Ferakis, N. and M. Stavropoulos, "Mini percutaneous nephrolithotomy in the treatment of renal and upper ureteral stones: Lessons learned from a review of the literature", *Urology Annals*, Vol. 7, No. 2, p. 141, 2015, https://doi.org/10.4103/0974-7796.152927.

48. Lahme, S., "Miniaturisation of PCNL", *Urolithiasis*, Vol. 46, No. 1, pp. 99–106, 2017, https://doi.org/10.1007/s00240-017-1029-3.

49. Bagcioglu, M., A. Demir, H. Sulhan, M. A. Karadag, M. Uslu and U. Y. Tekdogan, "Comparison of flexible ureteroscopy and micropercutaneous nephrolithotomy in terms of cost-effectiveness: analysis of 111 procedures", *Urolithiasis*, Vol. 44, No. 4, pp. 339–344, 2015, https://doi.org/10.1007/s00240-015-0828-7.

50. Aminsharifi, A., D. Irani, S. Pooyesh, H. Parvin, S. Dehghani, K. Yousofi, E. Fazel and F. Zibaie, "Artificial Neural Network System to Predict the Postoperative Outcome of Percutaneous Nephrolithotomy", *Journal of Endourology*, Vol. 31, No. 5, pp. 461–467, 2017, https://doi.org/10.1089/end.2016.0791.

51. Shabaniyan, T., H. Parsaei, A. Aminsharifi, M. M. Movahedi, A. T. Jahromi, S. Pouyesh and H. Parvin, "An artificial intelligence-based clinical decision support system for large kidney stone treatment", *Australasian Physical & Engineering Sciences in Medicine*, Vol. 42, No. 3, pp. 771–779, 2019, https://doi.org/10.1007/s13246-019-00780-3.

52. Johnston, W. K., R. K. Low and S. Das, "The evolution and progress of ureteroscopy", *Urologic Clinics of North America*, Vol. 31, No. 1, pp. 5–13, 2004, https://doi.org/10.1016/s0094-0143(03)00100-9.

53. Beiko, D. T. and J. D. Denstedt, "Advances in Ureterorenoscopy", *Urologic Clinics of North America*, Vol. 34, No. 3, pp. 397–408, 2007, https://doi.org/10.1016/j.ucl.2007.05.003.

54. Bagley, D., J. L. Huffman and E. Lyon, "Combined Rigid and Flexible Ureterg-pyeloscopy", *Journal of Urology*, Vol. 130, No. 2, pp. 243–244, 1983, https://doi.org/10.1016/s0022-5347(17)51083-6.

55. Bagley, D. H., J. L. Huffman and E. S. Lyon, "Flexible Ureteropyeloscopy: Diagnosis and Treatment in the Upper Urinary Tract", *Journal of Urology*, Vol. 138, No. 2, pp. 280–285, 1987, https://doi.org/10.1016/s0022-5347(17)43119-3.

56. Huang, Z., F. Fu, Z. Zhong, L. Zhang, R. Xu and X. Zhao, "Flexible Ureteroscopy and Laser Lithotripsy for Bilateral Multiple Intrarenal Stones: Is This a Valuable Choice?", *Urology*, Vol. 80, No. 4, pp. 800–804, 2012, https://doi.org/10.1016/j.urology.2012.05.013.

57. Somani, B., A. Srivastava, O. Traxer and O. Aboumarzouk, "Flexible ureterorenoscopy: Tips and tricks", *Urology Annals*, Vol. 5, No. 1, p. 1, 2013, https://doi.org/10.4103/0974-7796.106869.

58. Monga, M., K. J. Anderson and W. Durfee, "Physical Properties of Flexible Ureteroscopes: Implications for Clinical Practice", *Journal of Endourology*, Vol. 18, No. 5, pp. 462–465, 2004, https://doi.org/10.1089/0892779041271454.

59. Ozyuvali, E., B. Resorlu, U. Oguz, Y. Yildiz, T. Sahin, C. Senocak, O. F. Bozkurt, E. Damar, M. Yildirim and A. Unsal, "Is routine ureteral stenting really necessary after retrograde intrarenal surgery?", *Archivio Italiano di Urologia e Andrologia*, Vol. 87, No. 1, p. 72, 2015, https://doi.org/10.4081/aiua.2015.1.72.

60. Andonian, S., Z. Okeke and A. D. Smith, "Digital Ureteroscopy: The Next Step", *Journal of Endourology*, Vol. 22, No. 4, pp. 603–606, 2008, https://doi.org/10.1089/end.2008.0017.

61. Golden, J. P. and F. S. Ligler, "A comparison of imaging methods for use in an array biosensor", *Biosensors and Bioelectronics*, Vol. 17, No. 9, pp. 719–725,

2002, https://doi.org/10.1016/s0956-5663(02)00060-x.

62. User, H. M., V. Hua, L. W. Blunt, C. Wambi, C. M. Gonzalez and R. B. Nadler, "Performance and Durability of Leading Flexible Ureteroscopes", *Journal of Endourology*, Vol. 18, No. 8, pp. 735–738, 2004, https://doi.org/10.1089/end.2004.18.735.

63. Knudsen, B., R. Miyaoka, K. Shah, T. Holden, T. M. Turk, R. N. Pedro, C. Kriedberg, B. Hinck, O. Ortiz-Alvarado and M. Monga, "Durability of the Next-generation Flexible Fiberoptic Ureteroscopes: A Randomized Prospective Multi-institutional Clinical Trial", *Urology*, Vol. 75, No. 3, pp. 534–538, 2010, https://doi.org/10.1016/j.urology.2009.06.093.

64. Takayasu, H. and Y. Aso, "Recent Development for Pyeloureteroscopy: Guide Tube Method for Its Introduction into the Ureter", *Journal of Urology*, Vol. 112, No. 2, pp. 176–178, 1974, https://doi.org/10.1016/s0022-5347(17)59675-5.

65. Kourambas, J., R. R. Byrne and G. M. Preminger, "Does a ureteral access sheath facilitate ureteroscopy?", *Journal of Urology*, Vol. 165, No. 3, pp. 789–793, 2001, https://doi.org/10.1016/s0022-5347(05)66527-5.

66. Rukin, N., B. Somani, J. Patterson, B. Grey, W. Finch, S. Mcclinton, B. Parys, G. Young, H. Syed, A. Myatt, A. Samsudin, J. Inglis and D. Smith, "Tips and tricks of ureteroscopy: consensus statement Part I. Basic ureteroscopy", *Central European Journal of Urology*, Vol. 68, No. 4, pp. 439–446, 2015, https://doi.org/10.5173/ceju.2015.605a.

67. Rapoport, D., A. E. Perks and J. M. Teichman, "Ureteral Access Sheath Use and Stenting in Ureteroscopy: Effect on Unplanned Emergency Room Visits and Cost", *Journal of Endourology*, Vol. 21, No. 9, pp. 993–998, 2007, https://doi.org/10.1089/end.2006.0236.

68. Traxer, O. and A. Thomas, "Prospective Evaluation and Classification of Ureteral

Wall Injuries Resulting from Insertion of a Ureteral Access Sheath During Retrograde Intrarenal Surgery", *Journal of Urology*, Vol. 189, No. 2, pp. 580–584, 2013, https://doi.org/10.1016/j.juro.2012.08.197.

69. İbrahim Can Aykanat, *Retrograd İntrarenal Taş Cerrahisinde Kullanılan Üreteral Erişim Kılıfı Çap Farkının Postoperatif Dönemde Üreter Darlığı Üzerine Etkisi*, Ph.D. Thesis, T.C. Sağlık Bilimleri Üniversitesi Ankara Numune Sağlık Uygulama Ve Araştırma Merkezi, 2019.

70. Ulvik, Ø., T. Wentzel-Larsen and N. M. Ulvik, "A Safety Guidewire Influences the Pushing and Pulling Forces Needed to Move the Ureteroscope in the Ureter: A Clinical Randomized, Crossover Study", *Journal of Endourology*, Vol. 27, No. 7, pp. 850–855, 2013, https://doi.org/10.1089/end.2013.0027.

71. Atar, M., *Böbrek Ve Üreter Taşlarının Kontrastsız Bilgisayarlı Tomografi Üzerinde Hesaplanan Hounsfield Ünitesinin Holmium:Yag Laser İle Yapılan Üreterorenoskopi Ve Retrograd İntrarenal Cerrahi Tedavisinde Fragmantasyon Üzerindeki Etkisi*, Ph.D. Thesis, Bozok Üniversitesi Tıp Fakültesi Üroloji Anabilim Dalı, 2019.

72. Holden, T., R. N. Pedro, K. Hendlin, W. Durfee and M. Monga, "Evidence-Based Instrumentation for Flexible Ureteroscopy: A Review", *Journal of Endourology*, Vol. 22, No. 7, pp. 1423–1426, 2008, https://doi.org/10.1089/end.2007.0327.

73. *Böbreğe Takılan Çift J (Double J) Stentler Hakkında Bilgi*, 2020, https://www.doktortakvimi.com/blog/bobrege-takilan-cift-j-double-j-stentler-hakkinda-bilgi, accessed March 26, 2020.

74. Johnson, D. E., D. M. Cromeens and R. E. Price, "Use of the holmium:YAG laser in urology", *Lasers in Surgery and Medicine*, Vol. 12, No. 4, pp. 353–363, 1992, https://doi.org/10.1002/lsm.1900120402.

75. Sofer, M., J. D. Watterson, T. A. Wollin, L. Nott, H. Razvi and J. D. Denstedt,

"Holmium:YAG laser lithotripsy for upper urinary tract calculi in 598 patients.", *Journal of Urology*, Vol. 167, No. 1, pp. 31–34, 2002, https://doi.org/10.1016/s0022-5347(05)65376-1.

76. Pierre, S. and G. M. Preminger, "Holmium laser for stone management", *World Journal of Urology*, Vol. 25, No. 3, pp. 235–239, 2007, https://doi.org/10.1007/s00345-007-0162-y.

77. Önem, K., Öner Şanlı and T. Esen, "Ürolojide lazer kullanımı: Günümüzdeki durumu ve gelecekteki konumu.", *Türkiye Klinikleri J Urology-Special Topics*, Vol. 3, No. 1, pp. 12–19, 2010.

78. Aytekin, C., *Retrograd İntrarenal Cerrahi Yapılan Böbrek Taşı Hastalarında Taş Boyutu, Dansitesi Ve Lokalizasyonunun; Taşsızlık Ve Komplikasyon Oranlarına Etkisinin Karşılaştırılması*, Ph.D. Thesis, Mersin Üniversitesi Tıp Fakültesi Üroloji Anabilim Dalı, 2019.

79. Chawla, S. N., M. F. Chang, A. Chang, J. Lenoir and D. H. Bagley, "Effectiveness of High-Frequency Holmium:YAG Laser Stone Fragmentation: The "Popcorn Effect"", *Journal of Endourology*, Vol. 22, No. 4, pp. 645–650, 2008, https://doi.org/10.1089/end.2007.9843.

80. Santiago, J. E., A. B. Hollander, S. D. Soni, R. E. Link and W. A. Mayer, "To Dust or Not To Dust: a Systematic Review of Ureteroscopic Laser Lithotripsy Techniques", *Current Urology Reports*, Vol. 18, No. 4, p. 32, 2017, https://doi.org/10.1007/s11934-017-0677-8.

81. Torricelli, F., G. Marchini, R. Pedro and M. Monga, "Ureteroscopy for management of stone disease: An up to date on surgical technique and disposable devices", *Minerva urologica e nefrologica = The Italian journal of urology and nephrology*, Vol. 68, No. 6, pp. 516–526, 2016.

82. Bell, J. R., P. James, A. Rane and S. Y. Nakada, "International Holmium Laser

Lithotripsy Settings: An International Survey of Endourologists", *Journal of the American College of Surgeons*, Vol. 223, No. 4, p. e123, 2016, https://doi.org/10.1016/j.jamcollsurg.2016.08.307.

83. Hecht, S. L. and J. S. Wolf, "Techniques for Holmium Laser Lithotripsy of Intrarenal Calculi", *Urology*, Vol. 81, No. 2, pp. 442–445, 2013, https://doi.org/10.1016/j.urology.2012.11.021.

84. Schuler, T., M. Hasan and K. Pace, "Effect of holmium laser settings on stone fragmentation in vitro", *Can Urol Ass J*, Vol. 2, p. 251, 2008.

85. Teichman, J. M., G. J. Vassar, J. T. Bishoff and G. C. Bellman, "Holmium: YAG lithotripsy yields smaller fragments than Lithoclast, pulsed dye or electrohydraulic lithotripsy.", *Journal of Urology*, Vol. 159, No. 1, pp. 17–23, 1998, https://doi.org/10.1016/s0022-5347(01)63998-3.

86. Shah, O. and B. Matlaga, *Emerging Technologies in Renal Stone Management, An Issue of Urologic Clinics, Ebook*, The Clinics: Surgery, Elsevier Health Sciences, 2019, https://books.google.com.tr/books?id=BT6SDwAAQBAJ.

87. Corbin, N., J. Teichman, T. Nguyen, R. Glickman, L. Rihbany, M. Pearle and J. Bishoff, "Laser Lithotripsy and Cyanide", *Journal of endourology / Endourological Society*, Vol. 14, pp. 169–173, 2000.

88. Sea, J., L. M. Jonat, B. H. Chew, J. Qiu, B. Wang, J. Hoopman, T. Milner and J. M. Teichman, "Optimal Power Settings for Holmium:YAG Lithotripsy", *Journal of Urology*, Vol. 187, No. 3, pp. 914–919, 2012, https://doi.org/10.1016/j.juro.2011.10.147.

89. Finley, D. S., J. Petersen, C. Abdelshehid, M. Ahlering, D. Chou, J. Borin, L. Eichel, E. McDougall and R. V. Clayman, "Effect of Holmium:YAG Laser Pulse Width on Lithotripsy Retropulsion in Vitro", *Journal of Endourology*, Vol. 19, No. 8, pp. 1041–1044, 2005, https://doi.org/10.1089/end.2005.19.1041.

90. Kang, H. W., H. Lee, J. M. Teichman, J. Oh, J. Kim and A. J. Welch, "Dependence of calculus retropulsion on pulse duration during HO: YAG laser lithotripsy", *Lasers in Surgery and Medicine*, Vol. 38, No. 8, pp. 762–772, 2006, https://doi.org/10.1002/lsm.20376.

91. Lee, H., R. T. Ryan, J. M. Teichman, J. Kim, B. Choi, N. V. Arakeri and A. Welch, "Stone Retropulsion During Holmium:Yag Lithotripsy", *Journal of Urology*, Vol. 169, No. 3, pp. 881–885, 2003, https://doi.org/10.1097/01.ju.0000046367.49923.c6.

92. Mues, A. C., J. M. Teichman and B. E. Knudsen, "Quantification of Holmium:Yttrium Aluminum Garnet Optical Tip Degradation", *Journal of Endourology*, Vol. 23, No. 9, pp. 1425–1428, 2009, https://doi.org/10.1089/end.2009.0384.

93. *Lumenis Pulse Holmium Surgical Laser Operator's Manual*, 2017, https://prd-medweb-cdn.s3.amazonaws.com/documents/periopservices/files/UM-10012510_F\%20Lumenis\%20Pulse\%20120H\%20Op\%20Manual_English.pdf, accessed January 4, 2020.

94. Ito, H., S. Kuroda, T. Kawahara, K. Makiyama, M. Yao and J. Matsuzaki, "Preoperative factors predicting spontaneous clearance of residual stone fragments after flexible ureteroscopy", *International Journal of Urology*, Vol. 22, No. 4, pp. 372–377, 2015, https://doi.org/10.1111/iju.12690.

95. Tonyali, S., , M. Yilmaz, M. Karaaslan, C. Ceylan, L. Isikay, , and and, "Prediction of stone-free status after single-session retrograde intrarenal surgery for renal stones", *Türk Üroloji Dergisi/Turkish Journal of Urology*, Vol. 44, No. 6, pp. 473–477, 2018, https://doi.org/10.5152/tud.2018.88615.

96. Resorlu, B., A. Unsal, H. Gulec and D. Oztuna, "A New Scoring System for Predicting Stone-free Rate After Retrograde Intrarenal Surgery: The "Resorlu-Unsal Stone Score"", *Urology*, Vol. 80, No. 3, pp. 512–518, 2012, https://doi.

org/10.1016/j.urology.2012.02.072.

97. Jung, J.-W., B. K. Lee, Y. H. Park, S. Lee, S. J. Jeong, S. E. Lee and C. W. Jeong, "Modified Seoul National University Renal Stone Complexity score for retrograde intrarenal surgery", *Urolithiasis*, Vol. 42, No. 4, pp. 335–340, 2014, https://doi.org/10.1007/s00240-014-0650-7.

98. Akman, T., M. Binbay, F. Ozgor, M. Ugurlu, E. Tekinarslan, C. Kezer, R. Aslan and A. Y. Muslumanoglu, "Comparison of percutaneous nephrolithotomy and retrograde flexible nephrolithotripsy for the management of 2-4 cm stones: a matched-pair analysis", *BJU International*, Vol. 109, No. 9, pp. 1384–1389, 2011, https://doi.org/10.1111/j.1464-410x.2011.10691.x.

99. Breda, A., O. Ogunyemi, J. T. Leppert, J. S. Lam and P. G. Schulam, "Flexible Ureteroscopy and Laser Lithotripsy for Single Intrarenal Stones 2 cm or Greater—Is This the New Frontier?", *Journal of Urology*, Vol. 179, No. 3, pp. 981–984, 2008, https://doi.org/10.1016/j.juro.2007.10.083.

100. Xiao, Y., D. Li, L. Chen, Y. Xu, D. Zhang, Y. Shao and J. Lu, "The R.I.R.S. scoring system: An innovative scoring system for predicting stone-free rate following retrograde intrarenal surgery", *BMC Urology*, Vol. 17, No. 1, p. 105, 2017, https://doi.org/10.1186/s12894-017-0297-0.

101. Kronenberg, P. and B. Somani, "Advances in Lasers for the Treatment of Stones—a Systematic Review", *Current Urology Reports*, Vol. 19, No. 6, p. 45, 2018, https://doi.org/10.1007/s11934-018-0807-y.

102. XU, M., P. Watanachaturaporn, P. Varshney and M. Arora, "Decision tree regression for soft classification of remote sensing data", *Remote Sensing of Environment*, Vol. 97, No. 3, pp. 322–336, 2005, https://doi.org/10.1016/j.rse.2005.05.008.

103. James, G., D. Witten, T. Hastie and R. Tibshirani, "Classification", *Springer*

Texts in Statistics, pp. 127–173, Springer New York, 2013, https://doi.org/10.1007/978-1-4614-7138-7_4.

104. Pekel, E., "Estimation of soil moisture using decision tree regression", *Theoretical and Applied Climatology*, Vol. 139, No. 3-4, pp. 1111–1119, 2019, https://doi.org/10.1007/s00704-019-03048-8.

105. Colin, B., S. Clifford, P. Wu, S. Rathmanner and K. Mengersen, "Using Boosted Regression Trees and Remotely Sensed Data to Drive Decision-Making", *Open Journal of Statistics*, Vol. 7, No. 5, pp. 859–875, 2017, https://doi.org/10.4236/ojs.2017.75061.

106. Chen, T. and C. Guestrin, "XGBoost", *Proceedings of the 22nd ACM SIGKDD International Conference on Knowledge Discovery and Data Mining - KDD 16*, ACM Press, 2016, https://doi.org/10.1145/2939672.2939785.

107. Jain, A., *Complete Guide to Parameter Tuning in XGBoost with codes in Python*, 2016, https://www.analyticsvidhya.com/blog/2016/03/complete-guide-parameter-tuning-xgboost-with-codes-python/, accessed June 6, 2020.

108. Piramuthu, S., "Evaluating feature selection methods for learning in data mining applications", *European Journal of Operational Research*, Vol. 156, No. 2, pp. 483–494, 2004, https://doi.org/10.1016/s0377-2217(02)00911-6.

109. Azur, M. J., E. A. Stuart, C. Frangakis and P. J. Leaf, "Multiple imputation by chained equations: what is it and how does it work?", *International Journal of Methods in Psychiatric Research*, Vol. 20, No. 1, pp. 40–49, 2011, https://doi.org/10.1002/mpr.329.

110. Simoneau, G., *Multiple imputation using chained equations: Issues and guidance for practice*, https://pdfs.semanticscholar.org/fb9d/bfff9f4bfd90bfe1f09b48ce4929874fee12.pdf, accessed June 20, 2020.